The Journal of Immunology

RESEARCH ARTICLE | MAY 05 2023

Twist1–IRF9 Interaction Is Necessary for IFN-Stimulated Gene Anti-Zika Viral Infection FREE

Yuan You; ... et. al

J Immunol (2023) 210 (12): 1899–1912.
https://doi.org/10.4049/jimmunol.2300081

Twist1–IRF9 Interaction Is Necessary for IFN-Stimulated Gene Anti-Zika Viral Infection

Yuan You,* Esteban Grasso,*,† Ayesha Alvero,* Jennifer Condon,* Tanya Dimova,‡ Anna Hu,* Jiahui Ding,* Marina Alexandrova,‡ Diana Manchorova,‡ Violeta Dimitrova,‡ Aihua Liao,§ and Gil Mor*

An efficient immune defense against pathogens requires sufficient basal sensing mechanisms that can deliver prompt responses. Type I IFNs are protective against acute viral infections and respond to viral and bacterial infections, but their efficacy depends on constitutive basal activity that promotes the expression of downstream genes known as IFN-stimulated genes (ISGs). Type I IFNs and ISGs are constitutively produced at low quantities and yet exert profound effects essential for numerous physiological processes beyond antiviral and antimicrobial defense, including immunomodulation, cell cycle regulation, cell survival, and cell differentiation. Although the canonical response pathway for type I IFNs has been extensively characterized, less is known regarding the transcriptional regulation of constitutive ISG expression. Zika virus (ZIKV) infection is a major risk for human pregnancy complications and fetal development and depends on an appropriate IFN-β response. However, it is poorly understood how ZIKV, despite an IFN-β response, causes miscarriages. We have uncovered a mechanism for this function specifically in the context of the early antiviral response. Our results demonstrate that IFN regulatory factor (IRF9) is critical in the early response to ZIKV infection in human trophoblast. This function is contingent on IRF9 binding to Twist1. In this signaling cascade, Twist1 was not only a required partner that promotes IRF9 binding to the IFN-stimulated response element but also an upstream regulator that controls basal levels of IRF9. The absence of Twist1 renders human trophoblast cells susceptible to ZIKV infection. ***The Journal of Immunology*****, 2023, 210: 1899–1912.**

Tissue homeostasis depends on an efficient immune defense against pathogens, which requires a sufficient baseline sensing mechanism that can deliver prompt responses (1). In addition, once the infection is cleared, mechanisms that can resolve the resulting inflammation are also required to avert chronic inflammatory conditions that can lead to tissue damage (2–5).

Type I IFNs (IFN-α and IFN-β) are polypeptides produced by mucosal and immune cells, as well as by infected cells, that are able to induce an antimicrobial state by modulating the innate immune response and activating the adaptive immune system (6, 7). Type I IFNs are protective against acute antiviral infections and respond against bacterial infections, but this function can have deleterious consequences as observed in autoimmune diseases (8, 9). Type I IFN responses can be induced by both viral and bacterial pathogens, which are sensed by TLRs, NOD-like receptors, and RIG-I–like receptors (10, 11). Ligation of these receptors results in the expression of stimulator of IFN genes (STING) (12). The canonical type I IFN signaling is mediated by binding of IFN-α or IFN-β to the type I IFN–associated receptors (IFN-α/β receptor [IFNAR]), leading to activation of members of the JAK kinase family (13, 14) and production of several hundred IFN-stimulated genes (ISGs). Activated JAK kinases phosphorylate STAT1 and STAT2 (6, 15), leading to their phosphorylation, dimerization, and translocation to the nucleolus where they assemble with IFN regulatory factor 9 (IRF9) to form a three-molecule complex called ISG factor 3 (ISGF3) (6, 16). ISGF3 binds to a DNA sequence known as the IFN-stimulated response element (ISRE, YAGTTTC(A/T)YTTTYCC [17]), activating the transcription of ISGs, the primary effectors of type I IFN–mediated biological responses (18).

The signaling components of the canonical type I IFN pathway are ubiquitously expressed and thus allow fast and effective responses to infections, even in the presence of low levels of IFN-β (14, 19, 20). The mechanisms regulating the basal expression of ISGs are still not clearly understood.

Trophoblast cells are the main cellular component of the placenta and, among their multiple functions, they provide immunological protection to the fetus against infections, especially viral infections (21). Trophoblast cells express pattern recognition receptors such as TLRs, Nod receptors, and RIG-1–like receptors (22), localized in the cell surface or intracellularly, which allows them to detect bacterial and viral-derived factors (23–28). Upon activation of TLR4 or TLR3, trophoblast cell express type I IFN-β, which induces the

*C.S. Mott Center for Human Growth and Development, Wayne State University, Detroit, MI; †School of Science, University of Buenos Aires, Buenos Aires, Argentina; ‡Institute of Biology and Immunology of Reproduction "Acad. Kiril Bratanov," Bulgarian Academy of Sciences, Sofia, Bulgaria; and §Institute of Reproductive Health, Center for Reproductive Medicine, Tongji Medical College, Huazhong University of Science and Technology, Wuhan, P.R. China

ORCIDs: 0000-0002-7629-977X (E.G.); 0000-0002-6593-3595 (A.A.); 0000-0001-8665-4352 (T.D.); 0000-0001-7747-2071 (J.D.); 0000-0002-3939-4604 (M.A.); 0000-0002-5499-3912 (G.M.).

Received for publication February 1, 2023. Accepted for publication April 10, 2023.

This work was supported in part by the Division of Intramural Research, National Institute of Allergy and Infectious Diseases Grant 5R01AI145829-03, Eunice Kennedy Shriver National Institute of Child Health and Human Development Grant 1R01HD111146-01, and by National Institute of Environmental Health Sciences Grant 1P42ES030991-01A1 (to G.M.).

Conceptualization, G.M., Y.Y., and A.L.; methodology, Y.Y., E.G., J.C., T.D., A.H., J.D., M.A., D.M., and V.D.; RNA sequencing, Y.Y., E.G., A.H., and J.D.; writing—original draft, Y.Y.; writing—review and editing, A.A. and G.M.; supervision, G.M. and A.L.; and funding acquisition, G.M.

Address correspondence and reprint requests to Prof. Gil Mor, C.S. Mott Center for Human Growth and Development, Department of Obstetrics and Gynecology, Wayne State University, 275 East Hancock Street, Detroit, MI 48201. E-mail address: gmor@med.wayne.edu

The online version of this article contains supplemental material.

Abbreviations used in this article: BLS, blastocyst-like structure; DEG, differentially expressed gene; E, embryonic day; EVT, extravillous trophoblast; HLH, helix-loop-helix; IFNAR, IFN-α/β receptor; IRF9, IFN regulatory factor 9; ISG, IFN-stimulated gene; ISGF3, ISG factor 3; ISRE, IFN-stimulated response element; poly(I:C), polyinosinic-polycytidylic acid; qPCR, quantitative PCR; Sw.71, Swann71; TW-KO, Twist1-knockout; WT, wild-type; ZIKV, Zika virus.

expression a wide range of ISGs responsible for antiviral protection, immune regulation, and cell survival (10, 29).

We and others have shown the role of placental-derived IFN-β on the response to viral infections such as influenza, HSV2, and Zika virus (ZIKV) (10, 28, 30). The proper regulation of the antiviral response in the placenta is essential for the protection of the fetus and the mother (29). An excessive or dysregulated IFN-β response is responsible for fetal death or abnormal development of the fetus (10, 29, 31).

ZIKV is a mosquito-borne, positive-sense ssRNA virus belonging to the family Flaviviridae (genus *Flavivirus*). ZIKV infection is one the best examples where infection during early pregnancy has been associated with severe congenital defects (i.e., microcephaly) and pregnancy loss (32–34). Similar to other viruses, a successful ZIKV infection of trophoblast cells is based on the ZIKV capacity to inhibit the type I IFN response, an essential component of the protective antiviral response (35). The protective role of IFN-β against ZIKV has been demonstrated in IFN-β signaling–deficient mice, which lack the expression of ISGs and are highly susceptible to viral infection. However, the mechanism by which ZIKV is able to escape the type I IFN response has not been elucidated.

Twist1 is a transcription factor that regulates mesenchymal differentiation and cell motility (36) and has been reported to be downregulated in miscarriages (37). Much of our understanding of Twist1 function has been associated with developmental and cancer biology, although recent reports have shown that Twist1 may also regulate immune cell function. Twist1$^{+/-}$ mice demonstrate increased proinflammatory cytokines, associated with increased NF-κB signaling, perinatal death, and defects in type I IFN–mediated suppression of proinflammatory cytokines in macrophages (6, 38, 39), which is suggestive of a potential role of Twist1 on the type I IFN response to infections.

The objective of this study was to elucidate the molecular pathways responsible for maintaining the basal IFN response to infections and that could be targeted by viral infections, such as ZIKV. Our premise was that ZIKV, by modulating the type I IFN response, might affect trophoblast function. Using in vitro and in vivo models we identified Twist1 as a critical regulator of type I IFN signaling pathway by regulating IRF9 expression and function. Furthermore, we ascertain that Twist1 expression is inhibited as a result of the anti-ZIKV response, affecting trophoblast function.

Materials and Methods

Cell culture

Mycoplasma-free immortalized human trophoblast Swann71 (Sw.71) cells and human endometrial stroma cells were cultured in DMEM/F12 or DMEM supplemented with 10% FBS, 10 mm HEPES, 0.1 mm MEM nonessential amino acids, 1 mm sodium pyruvate, and 100 U/ml penicillin/streptomycin (Life Technologies, Waltham, MA) under 5% CO_2 at 37°C.

Viral infections were done as previously described (40, 41). In short, cells were seeded in six-well plates at 1.5×10^5 cells per well; the next day, ZIKV was added to the cells for a 1-h incubation (at the indicated multiplicity of infection) with gentle agitation every 20 min, and after 1 h, the inoculum was removed and the cells were washed twice with PBS, after which the cells were maintained in 10% FBS DMEM/F12 media for the duration of the experiment. At indicated time points postinfection, cell pellets and conditioned media were collected for downstream analysis.

Formation of blastocyst-like spheroids

Blastocyst-like structures (BLSs) were obtained as previously described (42, 43), In brief, first trimester trophoblast Sw.71 cells were trypsinized and then 4000 of these cells were added to each well of a Costar ultra-low attachment 96-well microplate (Corning, Corning, NY). Cells were incubated for 48 h until they achieved a compact morphology (spheroid). Morphology was monitored using the Incucyte ZOOM (Essen Biosciences, Ann Arbor, MI). The differential

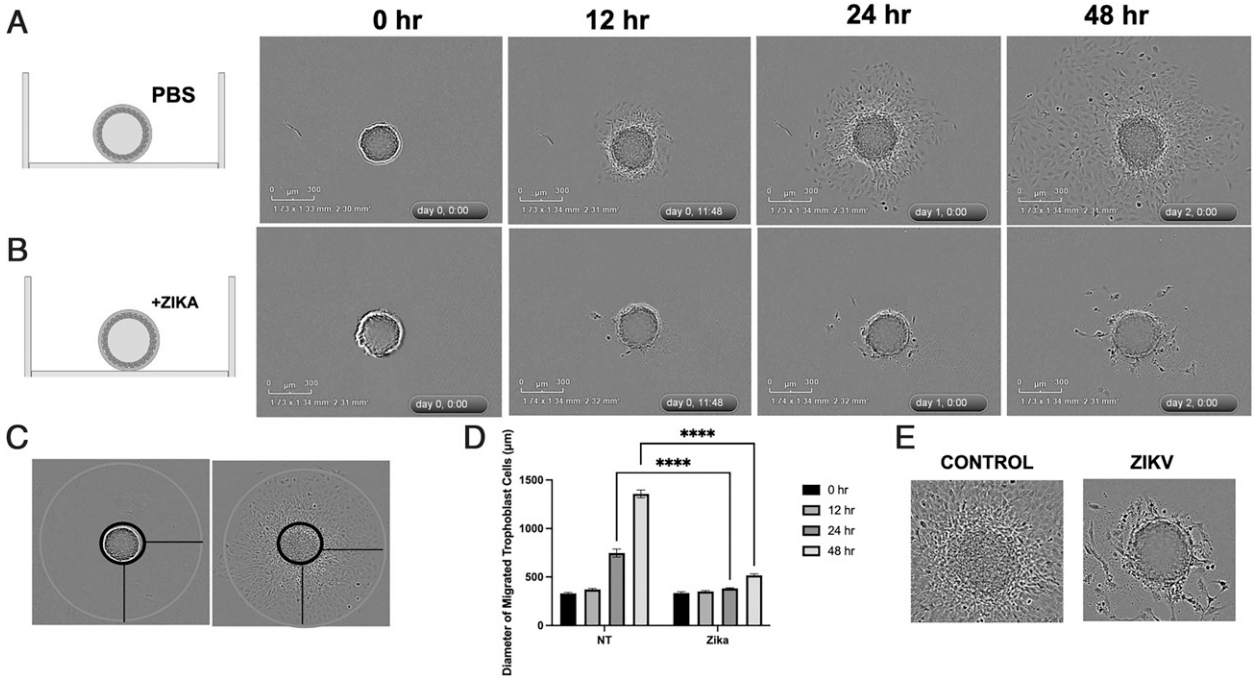

FIGURE 1. ZIKV infection inhibits trophoblast migration. Blastocyst-like structures (BLSs) were established from Sw.71 human first trimester trophoblast cells as described in *Materials and Methods* and exposed to ZIKV or vehicle control for up to 48 h. Trophoblast migration was monitored using live imaging. (**A**) Time-dependent migration of BLSs treated with vehicle. Note attachment to the plate and migration of trophoblast cells from BLSs. (**B**) Migration of BLSs treated with ZIKV. Note that BLSs exposed to ZIKV are able to attach but not migrate. Representative images are from 10 independent experiments, each in triplicate. (**C**) Method of quantification of trophoblast migration. Inner circle corresponds to the outline of attached BLSs. Outer circle corresponds to outline of migrating cells at the latest time point. Distance between the inner and outer circles are quantified (μm) and used as a measure of migration. (**D**) Quantification of trophoblast migration. Data are presented as mean ± SEM. $n = 10$ independent experiments, each one in triplicate. $^{****}p < 0.0001$. (**E**) Representative images of BLS migration comparing vehicle-treated and ZIKV-infected BLSs. NT, nontreatment.

cellular characteristics of trophoblast cells as a three-dimensional model or monolayer are described in detail elsewhere (43).

Knockout of Twist1 using CRISPR/Cas9

Twist1 was knocked out in the Sw.71 first trimester trophoblast cell line using CRISPR/Cas9. The guide RNA for ISG20 was designed using the CRISPR design tool from the Zhang Laboratory at the Massachusetts Institute of Technology (CRISPR.mit.edu) (44). Two DNA oligonucleotides were synthesized as follows: sense, 5′-TAGGCGGGAGTCCGCAGTCTTACG-3′; antisense, 5′-AAACCGTAAGACTGCGGACTCCCG-3′. Oligonucleotides were phosphorylated using T4 polynucleotide kinase and annealed by heating equimolar amounts to 95°C and cooling slowly to room temperature. This resulting guide was introduced to lentiCRISPRv2GFP plasmid using BsmBI restriction sites, and lentiCRISPRv2GFP was a gift from David Feldser (Addgene plasmid no. 82416) (45). Ten micrograms of the resulting plasmid was cotransfected with 8 μg of packaging plasmid pCMV-VSV-G and 4 μg of envelope plasmid psPAX2 in the presence of 60 μg of polyethylenimine (PEI) into HEK293T cells in a 100-mm dish. pCMV-VSV-G was a gift from Bob Weinberg (Addgene plasmid no. 8454) (46), and psPAX2 was a gift from Didier Trono (Addgene plasmid no. 12260). Then, packaged viral particles were collected by ultracentrifugation and were transduced into the Sw.71 cells. The cells were sorted based on the GFP expression. The deletion of Twist1was confirmed using the Sanger sequencing technique performed by GENEWIZ, and the overall efficiency was 91.1% as analyzed by TIDE (tracking of indels by decomposition). Protein expression was verified by Western blot.

Placenta samples

All human samples used in this study were obtained in accordance with the guidelines of the Declaration of Helsinki and approved by Human Research Ethics Committee at the University Obstetrics and Gynecology Hospital "Maichin Dom," Medical University, Sofia, Bulgaria (no. 250569/2018). Written informed consent was taken from all women. Healthy pregnant women in early pregnancy, directed to elective pregnancy termination (6–12 gestational weeks, $n = 20$), were involved in the study. Pregnancies complicated by clinical evidence of infection, steroid treatment, AIDS, alcohol abuse, and/or drug abuse and immune-associated diseases were excluded. Chorion samples were collected in sterile PBS and processed within 1 h.

Histology and immunohistochemistry

Early pregnancy trophoblast tissues (10 × 10 × 10 mm) were fixed in formalin-free HOPE fixative according to the manufacturer's recommendations (Innovative Diagnostik-System, Hamburg, Germany) and embedded in paraffin wax. The paraffin sections (5 μm) were routinely stained with H&E for histological investigation and then selected slides were subjected to immunohistochemistry for Twist staining using the three-step biotin–streptavidin enzyme method.

Tissue sections were deparaffinized and rehydrated through graded alcohol. Endogenous peroxidase activity was quenched by incubation in 3% hydrogen peroxide for 30 min at 37°C. To suppress nonspecific background staining the sections were blocked with Super Block (ScyTek Laboratories, Logan, UT). Rabbit anti-human polyclonal Ab against Twist1 (25465-1-AP, Proteintech) was applied to the sections for overnight incubation at 4°C in a humidified chamber. Then, the sections were processed with an UltraTek anti-polyvalent visualization system (ScyTek Laboratories, Logan, UT) according to the ScyTek kit protocol. The endogenous biotin was blocked with a biotin blocking kit (ScyTek Laboratories, Logan, UT). The peroxidase activity was revealed with ready-to-use 3,3′-diaminobenzidine tetrahydrochloride (DAB). Nuclei were slightly counterstained with hematoxylin. Between the incubations the slides were washed in PBS. Negative staining controls were performed by omitting the first Ab. Sections from human breast cancer tissue processed in the same way were used as positive controls for specificity of Twist staining.

Immunocytochemistry

Sw.71 and Sw.71-Twist1-knockout (TW-KO) cells as the monolayer and spheroids were used in this study. The characterization of these cells has been reported in numerous publications (47–49).

Three-dimensional Sw.71 models or two-dimensional Sw.71 monolayers were cultured for 24–48 h in sterile culture chambers on a glass slide (Falcon). The cells were fixed in 2% paraformaldehyde in PBS overnight at room temperature and stained for HLA-G and HLA-C using the indirect immunofluorescence method. After washing with PBS, the cells were incubated with Super Block (ScyTek Laboratories, Logan, UT) to suppress the nonspecific binding.

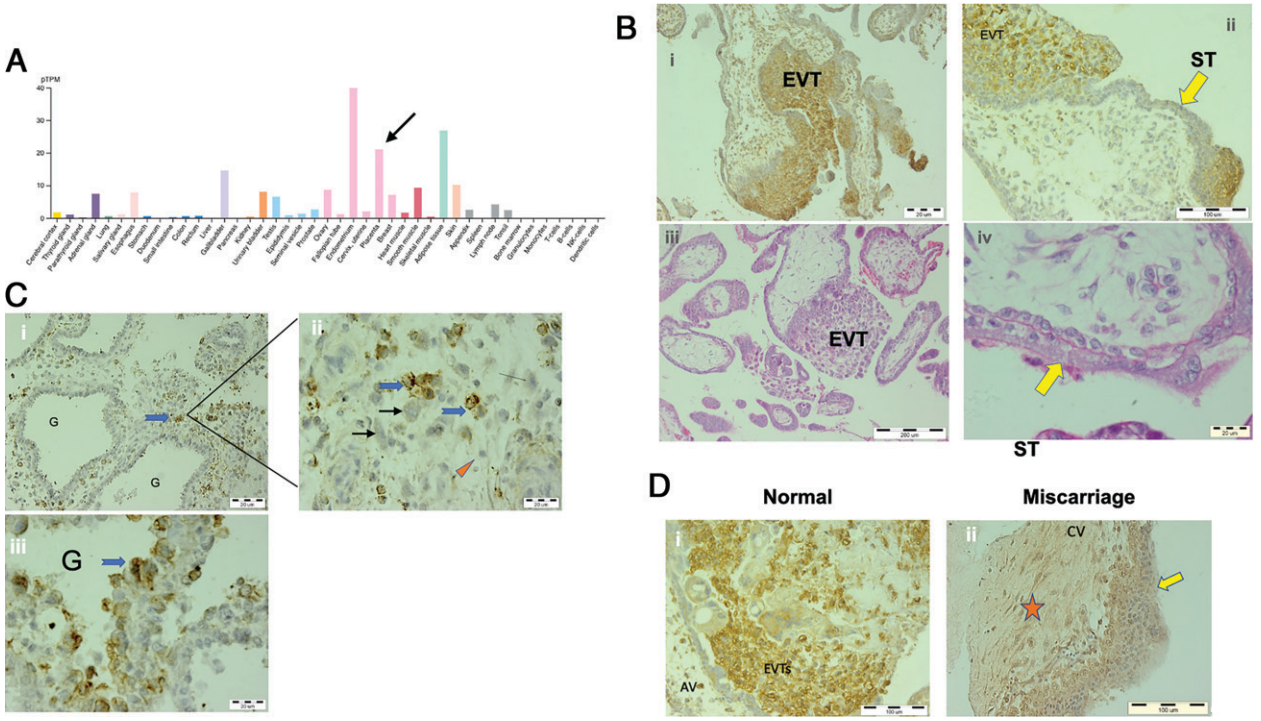

FIGURE 2. Twist expression in the human placenta. (**A**) Expression of Twist1 in human tissues (obtained from Human Protein Atlas). Note high expression in reproductive tissues such as ovary, endometrium, breast, and placenta. (**B**) Immunohistochemistry for Twist1 in first trimester human placentas. (**Bi**) Anchoring region EVT and (**Bii**) placental villi showed positive reactivity for Twist1. Cytotrophoblast and syncytiotrophoblast were negative. (**Biii**) H&E staining of anchoring region. (**Biv**) H&E staining of villi. Representative images are from $n = 12$ first trimester placentas. The yellow arrow points to the ST outside of the frame. (**C**) Blue arrows point to Twist1-positive EVT cells in decidua (**Ci** and **Cii**) and spiral arteries (**Ciii**); immune cells are Twist1-negative (red arrowhead). Representative images are from $n = 12$ first trimester placentas. The black arrows point to stroma cells. (**D**) Differential expression of Twist1 in placental samples obtained from elective termination (**Di**) and miscarriage (**Dii**). Note the decrease Twist expression in miscarriage samples. Representative images are from 12 normal placentas and six miscarriages. The yellow arrow points to the EVT and the orange star indicates the stroma. AV, anchoring village; CV, chorionic villi; G, glands; ST, syncytiotrophoblast.

As primary Abs we used anti-human rabbit polyclonal Abs against HLA-G (E-AB-18031, ScyTek Laboratories) and HLA-C (E-AB-17922, Elabscience) in appropriate dilutions for overnight incubation at 4°C. As a secondary Ab, goat anti-rabbit IgG conjugated with AF488 (E-AB-1055, Elabscience) was applied. Negative controls were prepared by omitting primary Ab and/or secondary Ab.

Luminex multiplex assay

For the in vivo study, mice serum samples were collected as previously described (40). Supernatants were collected from cell cultures, centrifuged, aliquoted, and stored until use. The samples were thawed only once immediately prior to running the assay. The samples were run on a Luminex multiplex assay (R&D Systems, Minneapolis, MN) as previously described (50) for the following cytokines and chemokines: IL-1α, IL-1β, IL-2, IL-3, IL-4, IL-5, IL-6, IL-9, IL-10, IL-12 (p40), IL-12 (p70), IL-13, IL-17A, Eotaxin, G-CSF, GM-CSF, IFN-γ, KC, MCP-1 (MCAF), MIP-1α, MIP-1β, RANTES, and TNF-α.

RNA isolation and quantitative RT-PCR analysis

Total RNA was harvested from Sw.71 cells or TW-KO cells using the Qiagen RNeasy mini kit and RNase-free DNase kit (Qiagen, Valencia, CA) according to the manufacturer's protocol. RNA samples were quantified using the NanoDrop One spectrophotometer (Thermo Fisher Scientific). The purity of the RNA was assessed through the A260/A280 and A260/A230 levels. Individual mRNA abundance was determined using TaqMan one-step RT-PCR procedures on the CFX Connect real-time system (Bio-Rad Laboratories). Primer/probe sets for TaqMan assays were purchased from Applied Biosystems (Thermo Fisher Scientific). Relative expression values for each gene were calculated using a standard curve and the reference gene peptidylprolyl isomerase B (PPIB). Transcript levels of specific cytokines and chemokines were measured in Sw.71 treated for 6 h with IFN-β. Assay data were analyzed using the ΔΔCt method with Bio-Rad CFX Manager 3.1 software.

RNA sequencing

RNA sequencing service was performed by GENEWIZ. Total RNA from Sw.71 and TW-KO cells were extracted using a Qiagen RNeasy mini kit following the manufacturer's instructions (Qiagen, Hilden, Germany) and quantified using a Qubit 2.0 fluorometer (Thermo Fisher Scientific, Waltham, MA), and RNA integrity was checked using TapeStation (Agilent Technologies, Palo Alto, CA). The RNA sequencing library was prepared using the NEBNext Ultra II RNA library prep kit for Illumina using the manufacturer's instructions (New England Biolabs, Ipswich, MA). Briefly, mRNAs were initially enriched with oligo(dT) beads. Enriched mRNAs were fragmented for 15 min at 94°C. First-strand and second-strand cDNA were subsequently synthesized. cDNA fragments were end repaired and adenylated at 3′ ends, and universal adapters were ligated to cDNA fragments, followed by index addition and library enrichment by PCR with limited cycles. The sequencing library was validated on the Agilent TapeStation (Agilent Technologies, Palo Alto, CA), and quantified by using a Qubit 2.0 fluorometer (Thermo Fisher Scientific, Waltham, MA) as well as by quantitative PCR (Kapa Biosystems, Wilmington, MA).

Sequencing. The sequencing libraries were multiplexed and clustered onto a flow cell. After clustering, the flow cell was loaded onto the Illumina HiSeq instrument according to the manufacturer's instructions. The samples were sequenced using a 2 × 150-bp paired-end configuration. Image analysis and base calling were conducted with the HiSeq control software. Raw sequence data (.bcl files) generated from Illumina HiSeq were converted into fastq files and demultiplexed using Illumina bcl2fastq 2.17 software. One mismatch was allowed for index sequence identification. After investigating the quality of the raw data, sequence reads were trimmed to remove possible adapter sequences and nucleotides with poor quality using Trimmomatic v0.36. The trimmed reads were mapped to the [SPECIES] reference genome available on Ensembl using the STAR aligner v2.5.2b. BAM files were generated because of this step. Unique gene

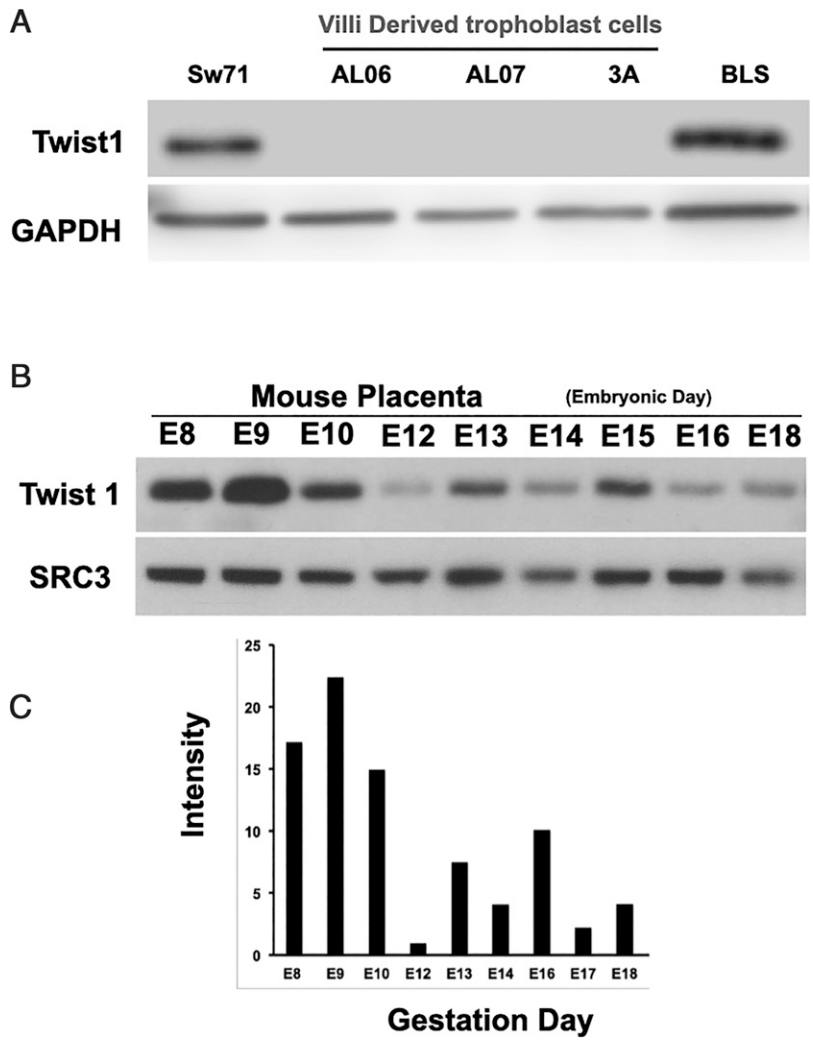

FIGURE 3. Twist1 expression in first trimester trophoblast cell lines. (**A**) Western blot analysis for Twist1 in cell lines Sw.71, ALO6, ALO7, and 3A and in BLSs. Note Twist1 positive expression only in Sw.71 and BLSs, which have migratory capacity. Representative figures are from three independent experiments. (**B**) Western blot shows temporal expression of Twist1 in mouse placenta. Placental samples were collected from pregnant mice from E8 to E18. Results are from a representative experiment of 15–18 placentas per time point obtained from three individual pregnant mice for each day. (**C**) Quantification of Twist1 expression in placental samples throughout pregnancy. Note the high levels of Twist1 protein expression during early placentation (E8–E10). Results are from a representative experiment of 15–18 placentas per time point obtained from three individual pregnant mice for each day.

hit counts were calculated by using feature Counts from the Subread package v1.5.2. Only unique reads that fell within exon regions were counted. After extraction of gene hit counts, the gene hit counts table was used for downstream differential expression analysis. Using DESeq2, a comparison of gene expression between the groups of samples was performed. The Wald test was used to generate p values and $\log_2$ fold changes. Genes with adjusted p values <0.05 and absolute $\log_2$ fold changes >1 were called as differentially expressed genes (DEGs) for each comparison. Gene Ontology analysis was performed on the statistically significant set of genes by implementing the software GeneSCF. The goa_[SPECIES] GO list was used to cluster the set of genes based on their biological process and determine their statistical significance.

Bioinformatics analysis

Differential expression analysis was performed in R using the linear modeling for microarray (limma) package (51, 52). Linear models were fitted to the protein abundance matrix with fetal sex, mother identity, and treatment considered as covariates. Limma implements an empirical Bayes-based moderated t statistic for significance analysis. For each experimental pair contrasted, proteins were considered differentially expressed when the corresponding p value was <0.05 and the $\log_2$ fold change was >0.6. Gene Ontology and pathway analyses were performed using the iPathwayGuide software from Advaita (53–56). Gene Ontology terms and Kyoto Encyclopedia of Genes and Genomes (KEGG) pathways were considered significantly enriched when the respective false discovery rate–adjusted p values was <0.05. Principal component analysis plots were generated using the pcaExplorer package (57), heatmaps were generated using the ComplexHeatmap package (58), and enriched Gene Ontology terms and pathways were graphed using the ggplot2 package (59) in R. The GOplot package was used to generate chord plots of the shown enriched Gene Ontology terms and constituent genes.

Luciferase assay

Sw.71 wild-type (WT) or TW-KO cells were transfected with the ISRE reporter kit plasmids (BPS Bioscience, San Diego, CA, catalog no. 60613) or cotransfected with either WT Twist1 plasmid or different Twist1 mutants in a 96-well plate using FuGENE 6 transfection reagent (Promega, Madison, WI, catalog no. E2691) according to the manufacturer's protocol. After transfection, the cells were incubated in culture medium for 24 h to allow for expression of the luciferase gene.

Statistical analysis

Statistical analyses were performed using Prism software, version 8 (GraphPad Software, San Diego, CA). All data are presented as means ± SEM. For mouse studies, a mixed-model ANOVA was used. When appropriate (when significance of a factor or of an interaction was established by the initial analysis), an analysis of the simple effect was performed using one-way ANOVA as needed. As needed, differences between two groups were analyzed using an unpaired Student t test and differences among multiple groups were analyzed by one-way ANOVA. Depending on the distribution of the continuous variables, a nonparametric test was used when the data were not normally distributed. A p value <0.05 was considered statistically significant.

Study approval

This study was carried out in accordance with the recommendations in the *Guide for the Care and Use of Laboratory Animals* of the National Institutes of Health. The protocols were approved by the Institutional Animal Care and Use Committee at the Wayne State University School of Medicine (assurance no. A3310-01).

Results

ZIKV infection inhibits trophoblast migration

The migration of trophoblast cells from the trophectoderm and subsequent invasion toward the endometrial stroma are critical steps in embryo implantation (60, 61). We questioned whether ZIKV infection could affect these processes. Thus, we used a previously reported in vitro system of three-dimensional BLSs formed from first trimester Swan71 trophoblast cells (42) (Fig. 1A). Under normal culture conditions, transfer of BLSs from ultra-low attachment conditions to tissue culture–treated wells showed attachment within 24 h and migration of trophoblast cells from the BLSs (Fig. 1B, 1C). However, pretreatment with ZIKV for 24 h prior to the transfer prevented BLS attachment and significantly inhibited trophoblast migration (Fig. 1B–E).

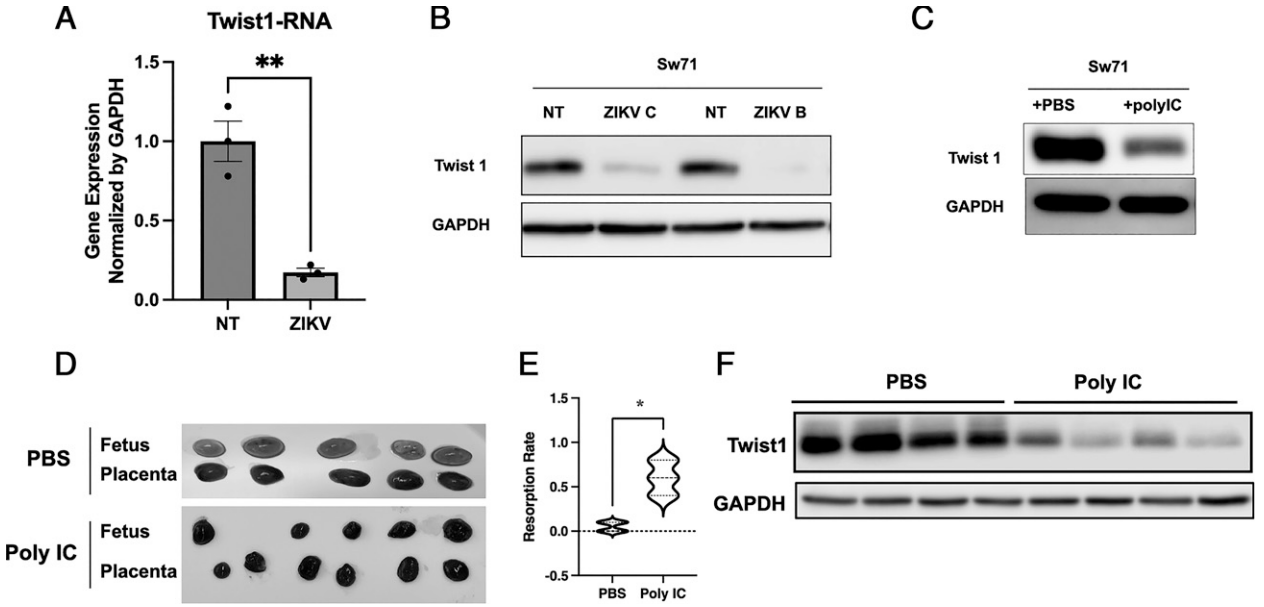

FIGURE 4. Effect of ZIKV infection on Twist1 expression in trophoblast cells. (**A**) Sw.71 first trimester trophoblast cell line was infected with ZIKV for 1 h and Twist1 mRNA was quantified by qPCR. Note significant decrease in Twist1 mRNA expression during ZIKV infection. $n = 6$ independent experiments in triplicate. $^{**}p < 0.01$. (**B**) Sw.71 first trimester trophoblast cell line was infected with ZIKV for 1 h and Twist1 protein levels were detected by Western blot. $n = 6$ independent experiments in triplicate. ZIKV B, Zika virus Brazil; ZIKV C, Zika virus Cambodia. (**C**) Sw.71 first trimester trophoblast cell line was treated with poly(I:C) or PBS control, and Twist1 protein levels were detected by Western blot. $n = 6$ independent experiments in triplicate. (**D**) Pregnant mice were injected with poly(I:C) on E14.5 and placental and fetal morphologies were evaluated 24 h later. Note placenta and fetus in the treated group. Results are representative of 24 placental samples. $n = 4$ mice per group. (**E**) Quantification of fetal resorption form experiment in (D). (**F**) Western blot analysis for Twist1 expression in placental samples from mice treated with poly(I:C). Note the decrease in Twist1 protein expression in placental samples from poly(I:C)-treated mice. Mice were injected on E14.5 and samples were collected at 4 h postinjection. $n = 5$ pregnant mice per group. Each mouse had an average of six to eight placentas.

These results show that ZIKV infection can prevent successful attachment and migration of BLSs in vitro.

Twist1 expression in placenta and trophoblast cells

Migration and invasion are accomplished by cells with mesenchymal phenotype. Twist1 is a transcription factor and master regulator of epithelial–mesenchymal transition (36) and has been reported to be downregulated in miscarriages (37). The Human Protein Atlas (https://www.proteinatlas.org/ENSG00000122691-TWIST1/tissue) showed that Twist1 is highly expressed in the placenta and endometrium (Fig. 2A). Thus, we stained first trimester human placentas to determine Twist1 cellular expression and observed cell-specific expression in extravillous trophoblast (EVT) but not the villi, syncytiotrophoblast, and cytotrophoblast (Fig. 2B). Twist1-positive EVT cells can be observed in the decidua and in close proximity to Twist1-negative decidual cells and immune cells (Fig. 2Ci, ii). We also identified Twist1-positive trophoblast cells within the glandular epithelium (Fig. 2Ciii). Interestingly, EVT cells in placental samples from miscarriages showed lower Twist1 expression compared with first trimester normal placenta (Fig. 2D).

We then evaluated Twist1 expression in monolayer cultures of established first trimester trophoblast cell lines (Swan71 and 3A) and primary cultures of villi-derived first trimester trophoblast (AL06 and AL07). We also evaluated Twist1 expression in the Swan71 BLSs. Similar to the findings in the placenta, AL06, AL07, and 3A showed no Twist1 expression; in contrast, Swan71 and its derived BLSs, which express the mesenchymal phenotype (42), were positive for Twist1 (Fig. 3A). Because EVTs are the trophoblast cells with migratory capacity, the specific expression of Twist1 in these cells further supports the role of Twist1 in trophoblast migration and invasion.

Mouse models are instrumental in increasing our knowledge of extraembryonic development, and although there are differences between human and mouse placentation, it still is a practical and accessible model to monitor the developmental process. Thus, we determined whether Twist1 expression is associated with the development of mouse placenta. We collected placental samples throughout gestation starting at embryonic day (E)8.5 (when placenta tissue is available) until E18.5 and examined Twist1 expression by Western blot. As shown in Fig. 3B, Twist1 expression is detectable in the mouse placenta although its expression varied along the gestation. We observed the highest expression around E8.5–E10.5 and lower expression at latter times (Fig. 3B, 3C). The high level of Twist1 during the E8.5–E10.5 period correlates with the process of trophoblast invasion and formation of the labyrinth that takes place in the mouse around this period (62, 63).

Cellular inflammatory response against viral signals inhibits Twist1 expression

Because we saw that ZIKV infection inhibits trophoblast migration, we examined whether it can affect Twist1 expression. Thus, Swan71 trophoblast cells were infected with ZIKV (Cambodia and Brazil strains) for 1 h and samples were collected at 48 h postinfection. Our data showed that infection with both ZIKV strains downregulated Twist1 expression both at the mRNA (Fig. 4A) and protein level (Fig. 4B).

To distinguish whether the inhibition of Twist1 is a direct result of ZIKV or a result of a cellular antiviral response due to the infection, we treated Swan71 trophoblast cells with polyinosinic-polycytidylic acid (poly(I:C)), a synthetic acid dsRNA, for 24 h. Similar to the results observed with ZIKV infection, poly(I:C) treatment inhibited Twist1 protein expression in vitro (Fig. 3C). To determine whether

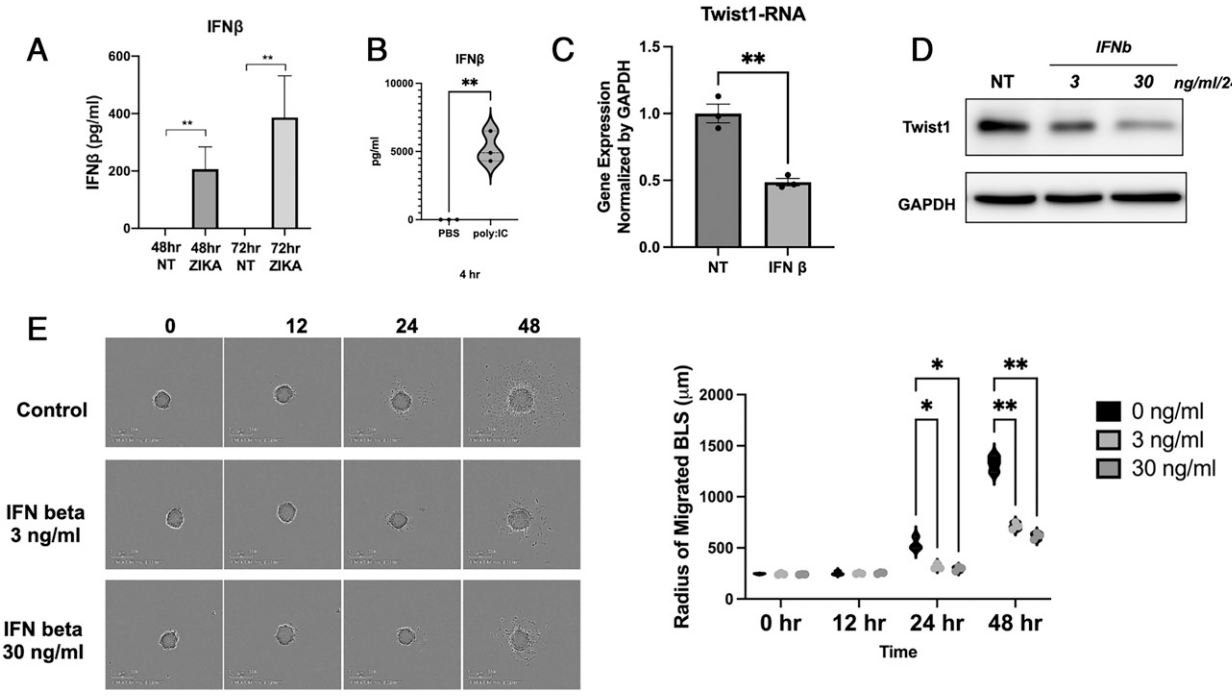

FIGURE 5. IFN-β induced by ZIKV infection inhibits Twit1 expression. (**A**) Sw.71 first trimester trophoblast cell line was infected with ZIKV for 48 and 72 h and IFN-β was quantified by ELISA. $n = 6$ independent experiments in triplicate. $^{**}p < 0.01$. (**B**) Sw.71 first trimester trophoblast cell line was treated with poly(I:C), and IFN-β was quantified by ELISA. $n = 6$ independent experiments in triplicate. $^{**}p < 0.01$. (**C**) Sw.71 first trimester trophoblast cell line was treated with IFN-β and Twist1 expression was measured by qPCR. $^{**}p < 0.01$. $n = 3$ independent experiments in triplicates. (**D**) Sw.71 first trimester trophoblast cell line was treated with IFN-β and Twist1 expression was measured by Western blot. Note the decrease on Twist expression following 24-h treatment with IFN-β. $n = 3$ independent experiments in triplicate. (**E**) BLSs were incubated in the presence of IFN-β (3 or 30 ng/ml) for 48 h. Trophoblast migration was monitored by live imaging. Representative image is from $n = 6$ independent experiments performed in triplicate.

this response also occurs in vivo, pregnant mice were treated with poly(I:C) at E8.5 (20 μg/kg). We saw the induction of pregnancy loss in poly(I:C)-treated mice within 24 h posttreatment (Fig. 4D, 4E) and analysis of placental samples at an earlier time point (4 h after poly(I:C)) showed a decrease in Twist1 expression. Taken together, these findings suggest that the antiviral response elicited from the trophoblast and not the ZIKV itself may be the regulatory mechanism that downregulates Twist1.

IFN-β inhibits Twist1 expression and trophoblast migration

A common cellular response to ZIKV infection and poly(I:C) treatment is the expression of type I IFN-β (Fig. 5A, 5B and Ref. 64). In vitro, we saw increased levels of IFN-β in Swan71 trophoblast cells following ZIKV infection (Fig. 5A), and in vivo, we could detect high levels of IFN-β in the serum of poly(I:C)-treated pregnant mice (Fig. 5B). We posit that cellular IFN-β, produced in response to viral infection, could be responsible for the decrease on Twist1 expression in the trophoblast. To test this hypothesis, we treated Swan71 trophoblast cells with IFN-β (30 ng/ml, 24 h). Detection of Twist1 mRNA by quantitative PCR (qPCR) showed that IFN-β treatment downregulates Twist1 mRNA expression (Fig. 5C). The decrease in Twist1 was validated at the protein level. Treatment of Swan71 trophoblast cells for 24 h with 3 or 30 ng/ml IFN-β showed a dose-dependent decrease in Twist1 expression. Moreover, treatment of Swan71 trophoblast cells with 30 ng/ml IFN-β for 2, 8, 16, and 24 h showed an initial increase in Twist1 expression at the early 2-h time point followed by a time-dependent decrease in Twist1 protein expression in the succeeding time points (Supplemental Fig. 1). The inhibitory effect of IFN-β on Twist1 is restricted to Twist1, as we observed increased expression of other ISGs such as Viperin, IFITM, or ISG15 (Supplemental Fig. 2).

To confirm the link between IFN-β–induced inhibition of Twist1 and trophoblast migration, we treated Swan71 BLSs with increasing concentrations of IFN-β (3 and 30 ng/ml) and monitored trophoblast attachment and migration by live imaging. As described above, BLSs attached to the plate within 24 h followed by trophoblast migration; however, in the presence of IFN-β, trophoblast attachment and migration were significantly inhibited (Fig. 5E). These results demonstrate that IFN-β exerts a major regulatory role in Twist1 expression and migration in trophoblast cells.

Twist1 is required for trophoblast migration and a successful antiviral response

To further demonstrate the role of Twist1 in trophoblast cell migration and the response to viral infection, we knocked out Twist1 in Swan71 trophoblast cells using CRISPR/Cas9 and generated Swan71 TW-KO (Fig. 6A). The specific sequence deleted on the Twist1 gene is shown in Fig. 6B. TW-KO cells were able to form BLSs; however, these cells lost the capacity to migrate and invade (Fig. 6C, 6D), demonstrating the requirement of Twist1 in trophoblast migration and invasion.

To determine the role of Twist1 in response to viral infection, monolayer cultures of WT Swan71 trophoblast cells and Swan71 TW-KO cells were infected with ZIKV. Surprisingly, we observed a significant increase in ZIKV titers in Swan71 TW-KO cells compared with WT Swan71 trophoblast cells (Fig. 7A). Furthermore, Swan71 TW-KO cells are more sensitive to ZIKV infection and undergo cell death at 48 h postinfection (Fig. 7B). In contrast, WT Swan71 maintained cell viability when infected with ZIKV (Fig. 7B).

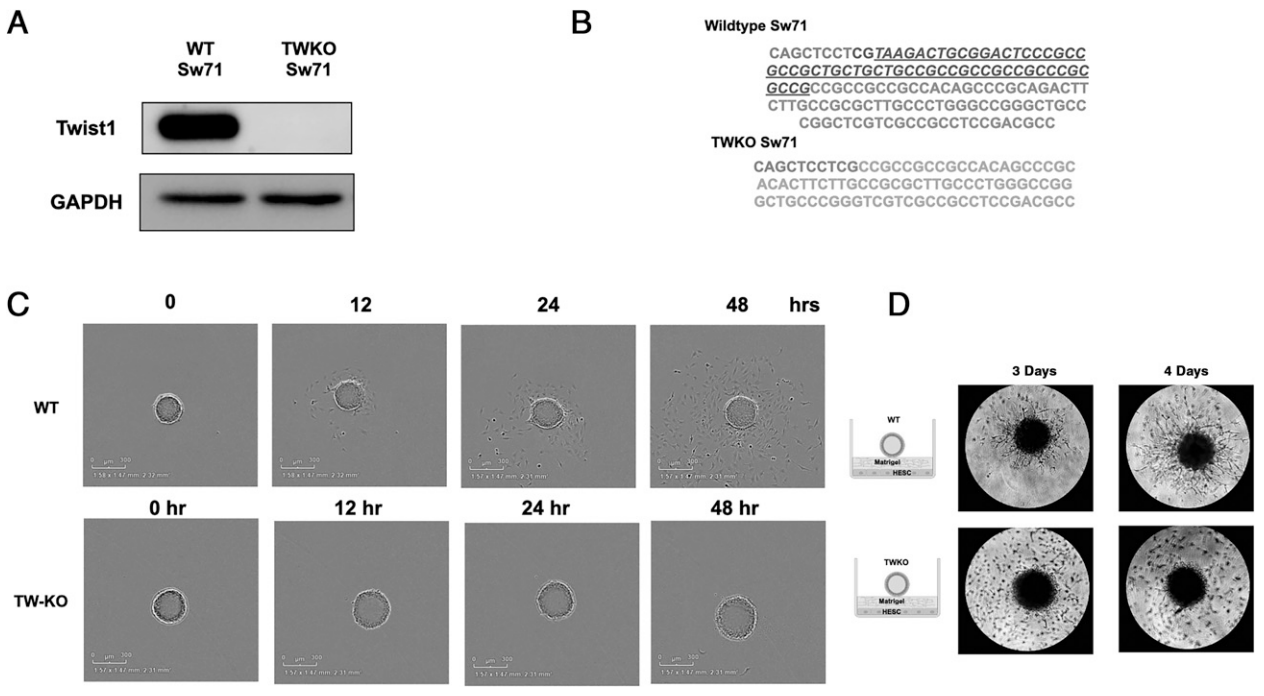

FIGURE 6. Characterization of a Twist1-deficient Sw.71 trophoblast cell line. (**A**) Twist1 was knocked out in a Sw71 first trimester trophoblast cell line using CRISPR/Cas9 as described in *Materials and Methods*. Western blot analysis for Twist1 expression in WT Sw.71 trophoblast cells and Twist-deficient clone (TW-KO) showed a successful Twist1 knockout. (**B**) Sequencing results showing WT Twist1 and deletion of Twist1 in TW-KO cells. The sequence targeted by guide RNA is shown italics and is underlined. The deleted sequence is shown in bold. (**C**) Migration assay comparing BLSs formed with Sw.71 WT and BLS formed with Sw.71 TW-KO cells. The representative image is from $n = 10$ independent experiments performed in triplicate. (**D**) In vitro model of trophoblast invasion. BLSs were transferred to wells containing stromal cells layered with Matrigel. WT Sw.71 trophoblast cells develop projections within the Matrigel, a sign of trophoblast invasion. No invasion was observed in BLSs formed with Sw.71 TW-KO cells. The representative image is from 10 independent experiments performed in triplicate.

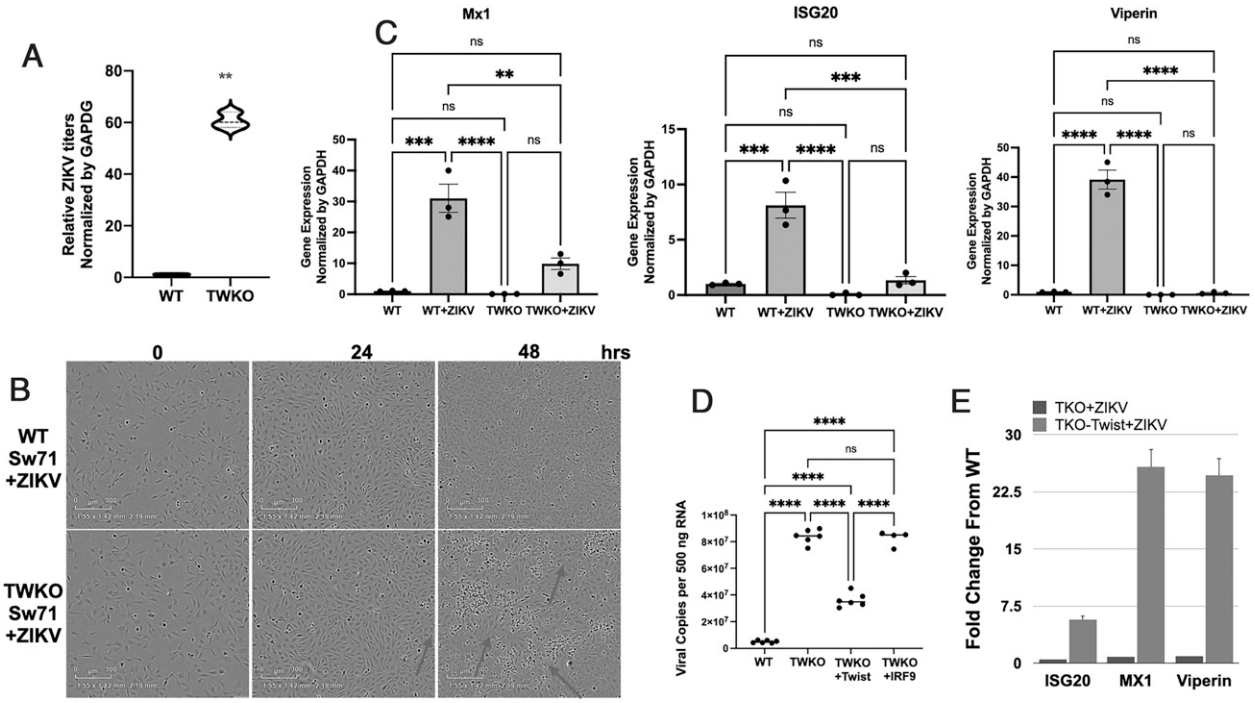

FIGURE 7. Sw.71 TW-KO cells are susceptible to ZIKV infection. (**A**) WT and Twist-KO Sw.71 trophoblast cells (TW-KO) were infected with ZIKV. Viral titers were determined by qPCR. Note the significant difference in viral titers between WT and Twist-KO. $n = 6$ independent experiments performed in triplicate. $^{**}p < 0.01$. (**B**) Twist-knockout Sw.71 trophoblast cells (TW-KO) undergo cell death following ZIKV infection. No cell death was observed in WT cells. Representative images are from six independent experiments performed in triplicate. (**C**) Wild type (WT) and Twist-KO Sw.71 trophoblast cells (TW-KO) were infected with ZIKV and expression levels of antiviral ISGs (Mx1, ISG20, and Viperin) were determined by qPCR. $n = 3$ independent experiments performed in triplicate. $^{**}p < 0.01$, $^{***}p < 0.001$, $^{****}p < 0.0001$. (**D**) Twist1 or IRF9 was overexpressed in Twist-KO Sw.71 trophoblast cells (TW-KO). Cultures were then infected with ZIKV and viral titers were quantified. Overexpression of Twist1 but not IRF9 restored the antiviral response. $n = 6$ independent experiments in triplicate. (**E**) Twist1 transcomplementation in Sw.71-KO cells reinstates the expression of ISGs in response to ZIKV infection. $n = 3$ independent experiments in triplicate. $^{****}p < 0.0001$.

Trophoblast cells control ZIKV infection through the expression of antiviral ISGs, such as ISG20, Mx1, ISG15, and Viperin, which can impede distinct steps in the viral cycle (10). As shown in Fig. 7C, ZIKV infection in WT Swan71 trophoblast cells triggers the expression of these ISGs; however, this response was significantly dampened in the Swan71 TW-KO cells (Fig. 7C).

To conclusively demonstrate the role of Twist1 in the cellular antiviral response we overexpressed Twist1 in Swan71 TW-KO followed by infection with ZIKV. The overexpression of Twist1 significantly decreased viral copy numbers compared with Swan71 TW-KO cells and was able to restore both the basal and antiviral levels of ISG20, Mx1, and Viperin (Fig. 7D, 7E). These findings demonstrate that Twist1 is not only necessary for trophoblast migration but also has an impact on the expression of antiviral ISGs necessary to control ZIKV infection.

Twist1 regulates basal levels of IRF9

To identify specific pathways and cellular processes regulated by Twist1 in trophoblast cells, we compared the transcriptome of WT Swan71 trophoblast cells and Swan71 TW-KO cells. We observed 644 upregulated genes and 1140 downregulated genes in the Swan71 TW-KO cells compared with the WT Swan71 trophoblast cells (Fig. 8A). Dendrogram analysis of differentially regulated biological processes using high-specificity pruning showed differential regulation of extracellular matrix organization, which explains the observed effect on trophoblast migration and invasion. More importantly, we observed that several processes related to viral response such as type I IFN signaling pathway, negative regulation of viral genome replication, and the defense response to viral infections were also differentially regulated in Swan71 TW-KO cells compared with WT Swan71 trophoblast cells (Fig. 8B). A closer analysis of DEGs in the type I IFN signaling pathway showed that most ISGs (Mx1, Mx2, XAF1, ISG15, ISG20, and IRF9) were downregulated in Swan71 TW-KO cells compared with WT Swan71 trophoblast cells (Fig. 8C). Network analysis of DEGs in the type I IFN signaling pathway showed IRF9 as the central regulator of this pathway downstream of Twist1 (Fig. 8D). The downregulation of IRF9 in Swan71 TW-KO cells was validated both at the protein level in total cell lysate (Fig. 9A) as well as on its cytoplasmic and nuclear fraction (Fig. 9B). Similarly, we observed a significant decrease on the basal levels of ISG20, ISG15, Mx1, and Viperin (Fig. 9C). It is noteworthy that nonclassical HLA-G, HLA-C, and HLA-F were also identified as significantly downregulated in Swan71 TW-KO cells compared with WT Swan71 trophoblast cells in the transcriptomic analysis (Fig. 8C). HLA-G and HLA-C are expressed in EVTs and have immune-suppressive function on immune cells, particularly NK cells (65, 66). Immunofluorescence analysis for HLA-G confirmed its basal expression in WT Swan71 trophoblast cells and decreased expression in Swan71 TW-KO cells (Fig. 9D). Taken together, these findings demonstrate that Twist1 expression has an impact on ISG expression in trophoblast cells.

Next, we sought to identify the specific mechanism by which Twist1 regulates the type I IFN signaling pathway in response to viral infection. We first determined changes in the expression of IFN-β or its receptor following ZIKV infection but did not observe any differences in the levels of IFN-β ligand and the IFNAR1 receptor between WT Swan71 trophoblast cells and Swan71 TW-KO cells both at baseline and with ZIKV (Supplemental Fig. 3),

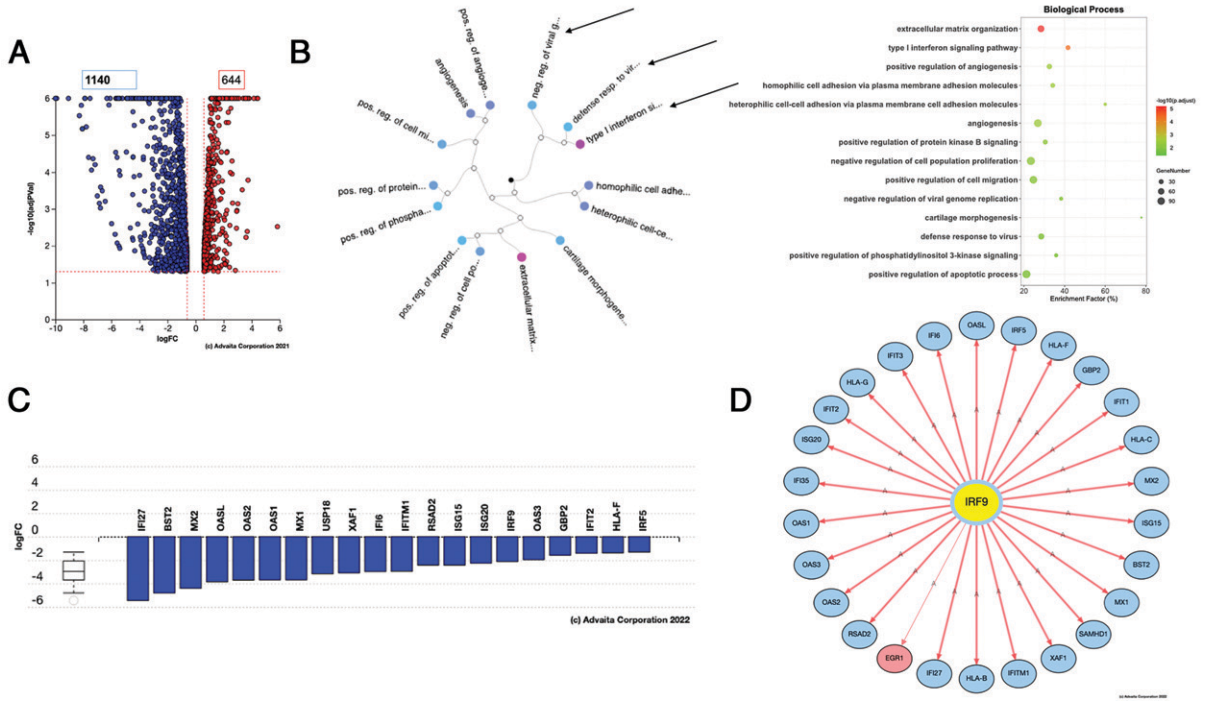

FIGURE 8. Knockout of Twist1 is associated with decreased ISG expression levels. (**A**) Volcano plot comparing WT Sw.71 cells and TW-KO cells (1140 genes were downregulated and 644 were upregulated in the TW-KO cells). Genes with a false discover rate–adjusted p value <0.05 and absolute $\log_2$ fold change >0.6 were considered differentially expressed. (**B**) Dendrogram of main biological processes affected by Twist1 knockout. Analysis was performed using high-specificity pruning. One of the top biological processes associated with the loss of Twist1 is type I IFN signaling. (**C**) Differentially expressed genes in the type I IFN signaling pathway comparing TW-KO cells and WT Sw.71 cells. Note that all of the differentially expressed genes were downregulated. (**D**) Network analysis of differentially expressed genes in the type I IFN signaling pathway comparing TW-KO cells and WT Sw.71 cells. Note that these differentially expressed genes are all regulated by IRF9.

demonstrating that the recognition of the virus and the production of IFN-β is Twist1-independent. We then evaluated the propagation of the signaling pathway downstream of IFN-β signaling (Fig. 10A). Thus, WT Swan71 trophoblast cells and Swan71 TW-KO cells were treated with IFN-β (30 ng/ml) for 2 h and levels of p-STAT1 and p-STAT2, which are the two main mediators of the canonical IFN-β signaling pathway (67), were determined by Western blot. We saw the upregulation of p-STAT1 and p-STAT2 in both the WT Swan71 trophoblast cells and Swan71 TW-KO cells (Fig. 10B). The increase on p-STAT1 and p-STAT2 following IFN-β treatment was time-dependent, peaking at ∼16 h after IFN-β treatment (Supplemental Fig. 1) in both the WT Swan71 trophoblast cells and Swan71 TW-KO cells. We did not observe the presence of p-STAT1 or p-STAT2 in the control group, nor the WT or KO cells (Supplemental Fig. 1). These findings suggest that the effect of Twist1 on the IFN-β signaling pathway is downstream of STAT phosphorylation.

As stated above, IRF9 was downregulated in Swan71 TW-KO cells compared with WT Swan71 trophoblast cells, in the cytoplasm as well as in the nucleus (Fig. 9B), and Twist1 is mainly expressed in the nucleus in WT Swan71 cells but is not detected in the KO cells (Fig. 9B). The lower levels of IRF9 in the Swan71 TW-KO cells, however, did not affect the nuclear translocation of p-STAT1 and p-STAT2 upon INF-β treatment (Fig. 10C). However, analysis of ISGs, which are more downstream in the pathway, showed that only the WT Swan71 trophoblast cells and not Swan71 TW-KO cells were able to upregulate the ISGs Mx1 and ISG20 in response to IFN treatment (Fig. 10B). Taken together, these results demonstrate that the critical node controlled by Twist1 in the IFN-β pathway is the basal level of IRF9.

Protein–protein interaction between Twist1 and IRF9

We then determined whether overexpression of IRF9 in Swan71 TW-KO cells would be sufficient to restore the capacity to control ZIKV replication. Thus, Swan71 TW-KO cells were stably transfected with pIRF9OE plasmid and infected with ZIKV. Despite the successful overexpression of IRF9 (Fig. 10D) and in contrast to the overexpression of Twist1, these cells were not able to control ZIKV replication any better than Swan71 TW-KO cells (Fig. 7D).

We further tested whether Twist1 can modulate IRF9 interaction with the ISRE by using an ISRE luciferase reporter system. This reporter contains a firefly luciferase gene under the control of multimerized ISRE responsive elements located upstream of a minimal promoter. The ISRE reporter is premixed with constitutively expressing *Renilla* luciferase vector, which serves as an internal control for transfection efficiency (Supplemental Fig. 4).

Transfection of the ISRE luciferase reporter system in WT Swan71 trophoblast cells showed luciferase activity, which was significantly downregulated in Swan71 TW-KO cells (Fig. 11A). Interestingly, overexpression of IRF9 alone or Twist1 alone in Swan71 TW-KO cells did not rescue the luciferase activity on the ISRE (Fig. 11A). Conversely, coexpression of Twist1 and IRF9 in Swan71 TW-KO cells was able to rescue luciferase activity in the ISRE similar to the levels observed in WT Swan71 trophoblast cells (Fig. 11A). These results indicate that without Twist1, IRF9 is not enough to control ZIKV infection. These findings place Twist1 as part of the IRF9 protein complex necessary for an early antiviral response.

Twist1 can directly bind the DNA at a conserved E-box motif or other transcriptional regulators and control their actions on the promoter. To determine whether the regulatory role of Twist1 in the

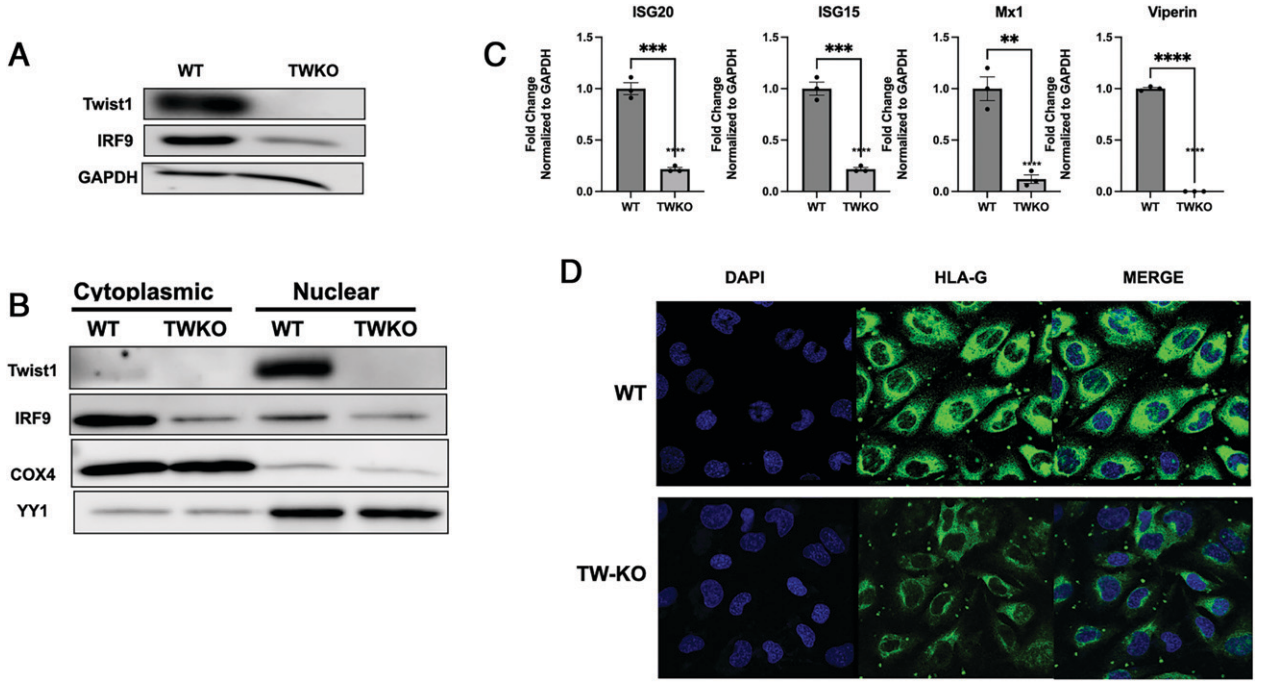

FIGURE 9. Inhibition of IRF9 basal expression in TW-KO cells. (**A**) Expression of Twist1 and IRF9 were determined by Western blot analysis in WT Sw.71 cells and TW-KO cells. Note the reduction in IRF9 levels in TW-KO cells. Results are representative of $n = 3$ independent experiments. (**B**) Cellular location of Twist1 and IRF9 were determined by nuclear/cytoplasmic fractionation. Twist1 is mainly localized in the nuclei of WT cells and is absent in TW-KO cells. IRF9 is mainly localized in the cytoplasm of WT cells and reduced TW-KO cells. COX4 and YY1 are markers for the purity of the fractions. COX4 cytoplasmic, YY1 nucleus. Results are representative of $n = 3$ independent experiments. (**C**) ISG20, ISG15, Mx1, and Viperin were quantified in WT Sw.71 cells and TW-KO cells by PCR. Note the significant decrease in TW-KO cells compared with WT Sw.71 cells. $n = 3$ independent experiments. $^{**}p < 0.01$, $^{***}p < 0.001$, $^{****}p < 0.0001$. (**D**) HLA-G expression in WT Sw.71 cells and TW-KO cells by immunofluorescence. HLA-G expression is a characteristic of EVTs and it is highly expressed in WT Sw.71 cells but is highly reduced in TW-KO cells. Results are representative of $n = 3$ independent experiments.

ISRE depends on its interaction with the DNA, we used several constructs of Twist1 with specific deletions and tested their effect on the ISRE luciferase reporter system (Fig. 11B). We first tested the Δhelix-loop-helix (HLH) construct, which has a deletion in the DNA-binding domain, and compared its effect on the ISRE reporter with full-length Twist1. As shown above, cotransfection of IRF9 with full-length Twist1 rescued luciferase activity in the ISRE. Interestingly, cotransfection of IRF9 with ΔHLH in Swan71 TW-KO cells was also able to rescue the activity of luciferase on the ISRE reporter (Fig. 11C). Because the reporter system does not contain an E-box sequence, these results demonstrate that direct binding to the E-box is not required for Twist1 to regulate ISG levels and suggest that protein–protein interaction may be the mechanism by which Twist1 regulates ISGs.

To test this hypothesis, we cotransfected IRF9 with Δ29–119, Δ51–82, and ΔWR, which are constructs with deletions in the Twist1 domains necessary for interaction with other proteins. Deletion of these domains failed to rescue the activity of luciferase on the ISRE reporter (Fig. 11C). Given that these domains are important for protein–protein interaction, these results further suggest that Twist1–IRF9 protein interaction is necessary for Twist1's activity on the ISRE

To further validate this hypothesis, we overexpressed both myc-tagged Twist1 and Flag-tagged IRF9 and performed immunoprecipitation to determine whether Twist1 binds IRF9. First, we immunoprecipitated myc and immunoblotted for IRF9. Analysis of the isolated immunocomplex demonstrated the presence of IRF9 (Fig. 11D). Similarly, when we immunoprecipitated for Flag and blotted for Twist1, we observed Twist1 in the isolated immunocomplex (Fig. 11D), further confirming that Twist1 binds IRF9. We did not detect the presence of p-STAT1 or p-STAT2 in the immunoprecipitated complex (Supplemental Fig. 4B). Taken together, our results demonstrate that Twist1, by binding to IRF9, is able to control IRF9 basal expression, a step necessary for the response to ZIKV infection (Fig. 12).

Discussion

Our study uncovered the mechanisms by which the Twsit1-IRF9 complex is able to provide an early antiviral response. IRF9 is a transcription factor that mediates the type I IFN response (6, 68). Ligation of IFNAR by type I IFNs results in the phosphorylation and dimerization of STAT1 and STAT2 (68). This dimer then recruits IRF9 to form the ISGF3 complex in cytoplasm. ISGF3 then translocates to the nucleus and binds to the ISRE, leading to the transcription of ISGs (69). IRF9 has also been shown to regulate cell proliferation (68), tumor formation (70), cardiovascular disease (71), inflammation (72), and immune cell regulation (73) independent of the ISGF3 complex. However, the mechanisms that allow IRF9 to function outside of the ISGF3 complex is not well understood. Our data, to our knowledge, provides a novel model where IRF9 in conjunction with Twist1 provides a continue and effective basal protection. However, upon recognition of viral factors by pattern recognition receptors, IFN-β expression is induced and activates the IFNAR pathway, which promotes Twist1 dissociation from the IRF9 complex, allowing the strong response mediated by the most efficient ISGF3 complex (Fig. 12).

We have uncovered a mechanism for this function specifically in the context of the early antiviral response. Our results demonstrate that Twist1 was not only a required partner that promotes IRF9 binding to ISRE but also an upstream regulator that controls basal levels

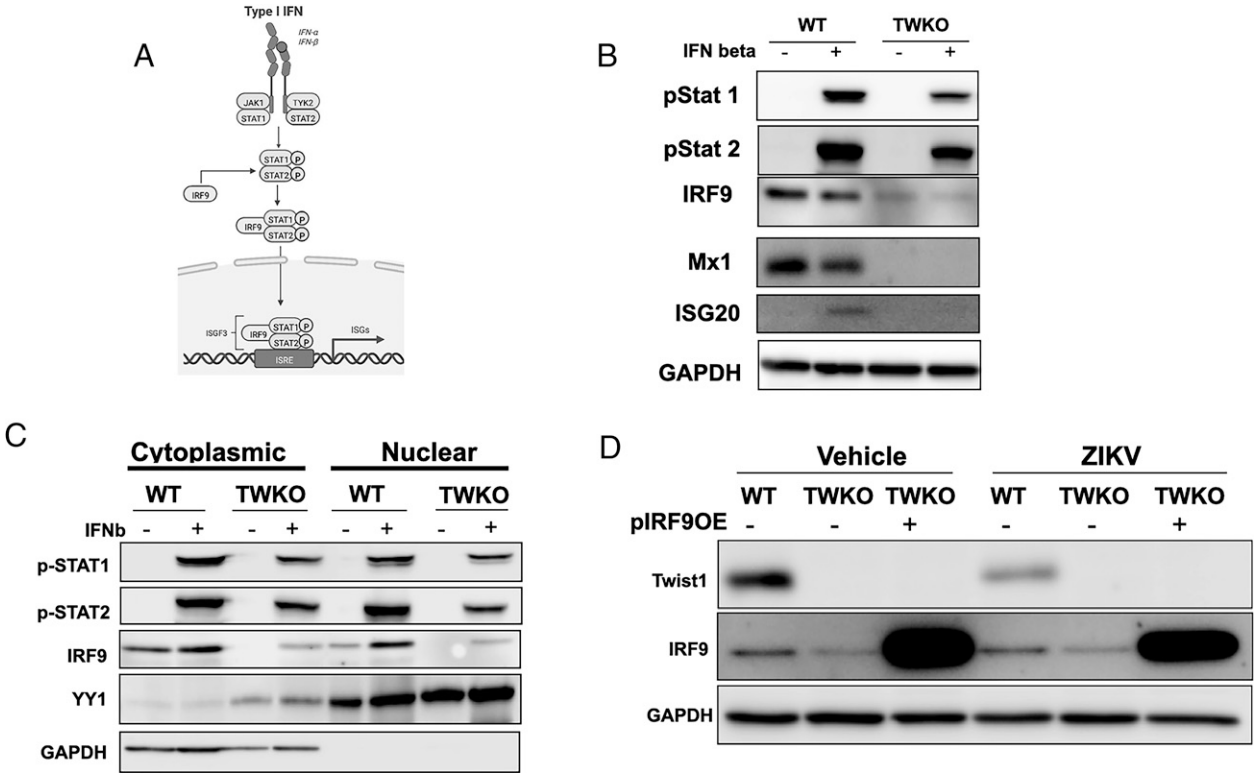

FIGURE 10. Integrity of the type I IFN-β canonical pathway. (**A**) Schematic representation of the canonical IFN-β pathway. (**B**) WT Sw.71 cells and TW-KO cells were treated with IFN-β, and activation of the canonical IFN-β pathway was determined by Western blot. Note the phosphorylation of STAT1 and STAT2 in both WT and TW-KO cells, but IRF9, Mx1, and ISG20 were only detected in WT Sw.71 cells. Results are representative of $n = 3$ independent experiments. (**C**) Nuclear and cytoplasmic fractionation in WT Sw.71 cells and TW-KO cells following IFN-β treatment. Note the nuclear translocation of p-STAT1 and p-STAT2 in both WT Sw.71 cells and TW-KO cells, but nuclear IRF9 is only detected in WT Sw.71 cells following IFN-β treatment. Results are representative of $n = 3$ independent experiments. (**D**) Overexpression of IRF9 in WT Sw.71 cells and TW-KO cells infected with ZIKV. Results are representative of $n = 3$ independent experiments.

of IRF9. Deletion of Twist1 decreases IRF9 mRNA and other ISGs, impairing the initial antiviral response in infected cells.

Interestingly, although the loss of Twist1 led to decreased basal IRF9 and ISG levels, it did not affect the canonical response to type I IFN. In Twist1-deficient cells, IFN-β maintained the ability to lead to phosphorylation of STAT1 and STAT2, to promote nuclear translocation of ISGF3, and to induce a significant increase in expression of ISGs. Consequently, we postulate that Twist1 is an additional mechanism necessary to maintain the basal expression of IRF9/ISGs in the absence type I IFN or in the presence of low levels of IFN-β.

Basal expressions of IRF9 and ISGs are essential to maintain a state of "readiness" to combat infection. By itself, IRF9 has low affinity to ISREs and therefore requires additional transcriptional factors to improve DNA binding (74, 75) and transcriptional activity (68). Our data demonstrate that Twist1 promotes IRF9 binding to DNA.

IRF9-Twist1 binding requires an intact C-terminal component of Twist1. Deletion of the WR domain but not the HLH domain (DNA-binding domain) of Twist1 inhibited the capacity to bind IRF9 and to enhance ISRE activity. Based on these findings we postulate that Twist1 interacts with IRF9 in the nucleus and increases IRF9 transcriptional efficacy for ISRE regulated genes. This interaction ensures the basal expression of ISGs, which is essential for the early protection against viral infections.

The importance of this basal expression is exemplified during viral infections such as ZIKV. Viral infections during pregnancy can have various outcomes ranging from no consequence to spontaneous abortion or successful birth but with associated congenital viral syndromes (30, 76–78). The outcome seems to be dictated by the gestational timing of the infections, with early infections being associated with pregnancy loss and fetal demise (32, 79, 80).

The placenta is an extraembryonic organ that ensures an appropriate supply of nutrients and oxygen to the fetus. In addition to this, it provides immunological protection and, as such, is a critical regulator of fetal growth and development. The formation of the placenta takes place during the early stages of embryo implantation and is the result of the migration of trophoblast cells from the trophectoderm and its invasion into the maternal endometrial/decidual tissue. The process of trophoblast migration and invasion is essential for the success of the pregnancy and is supported by maternal factors produced by decidual cells (81, 82). There are many ethical challenges in the study of human implantation, but the use of in vitro models that mimic the biological components of human implantation has overcome some of these limitations. In this study we used a well-characterized model that mimics, with its clear limitations, the capacity of the human trophoblast to migrate and invade (42, 43), and we showed that ZIKV infection perturbs trophoblast migration. We postulate that by affecting trophoblast migration, ZIKV infection during early pregnancy may lead to miscarriage. Indeed, pregnancy loss in women changes as gestational age advances, with a rate of ~25% at 45 wk, 2% at 20 wk, and 0.1% after 20 wk of gestation (83). In cases infected with ZIKV, it was reported that a 5.8% miscarriage rate and a 1.6% stillbirth rate occur when the women are infected during the first trimester (84).

Unexpectedly, we found that the impact of ZIKV infection on trophoblast migration was due to the antiviral response it generates, which is characterized by the expression of type I IFN-β and

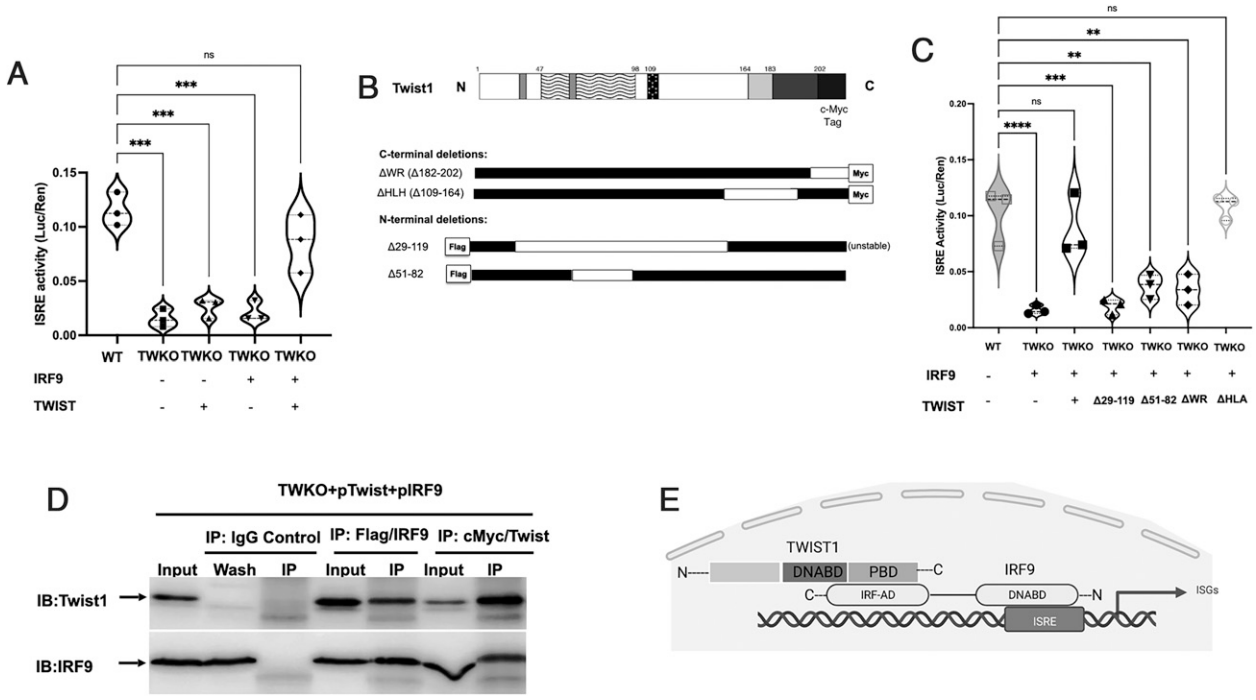

FIGURE 11. ISRE transcriptional activity in WT Sw.71 cells and TW-KO cells. (**A**) ISRE/luciferase (Luc)/Renilla (Ren) reporter system was transfected in WT Sw.71 cells and TW-KO cells together with IRF9 and/or Twist1 as indicated. Note the significant decrease in ISRE activity in TW-KO cells, which was rescued with cotransfection of IRF9 and Twist1. $n = 3$ independent experiments performed in triplicate. $^{***}p < 0.001$. (**B**) Schematic illustration of Twist1 protein and the deletions used to identify the domain required for binding to IRF9. Twist1 N-terminal deletion mutants have a Flag tag and C-terminal deletions have a Myc tag. (**C**) ISRE activity was measured in TW-KO cells transfected with IRF9 and different Twist1 constructs as indicated. Transcriptional activity is observed following cotransfection with IRF9 and Twist. Deletions at the N-terminal and the WR domain but not at the HLH domain are associated with loss of transcriptional activity. WT cells are used as a positive control. $n = 3$ independent experiments done in triplicate. $^{**}p < 0.01$, $^{***}p < 0.001$, $^{****}p < 0.0001$. (**D**) TW-KO cells were cotransfected with Twist and IRF9. Whole-cell lysates were used to immunoprecipitate the corresponding tag on Twist1 and IRF9, and immunoprecipitated complexes were probed to detect the presence of Twist and IRF9. IgG was used as control for all immunoprecipitates. Representative data are from three independent experiments. (**E**) Proposed model for Twist1 and IRF9 interaction. See text for details.

downstream ISGs. Indeed, treatment with IFN-β replicated ZIKV infection-induced inhibition of trophoblast attachment and migration.

Although mostly characterized for their ability to interfere with viral replication, IFNs, through specific ISGs, have immunomodulatory, cell differentiation, antiangiogenic, and proapoptotic effects (85). When left unchecked, the deleterious effects have been shown to produce complications such as autoimmune diseases, which have been associated with excessive or chronic type I IFN responses (3, 18, 19). Therefore, regulation of the type I IFN response is critical for an efficient immune response and maintenance of tissue homeostasis. We observed that the high levels of IFN-β expression in response to ZIKV infection had a detrimental effect on trophoblast function, and consequently we sought to identify the mechanism associated with this effect.

Interestingly, the most predominant gene affected by viral infection was Twist1, a highly evolutionally conserved basic HLH transcriptional factor that functions as a master regulator of gastrulation and mesodermal development (86–89). In addition to its role in embryogenesis, Twist1 has been found to be a key regulator in the inflammatory processes by functioning as a regulator of the NF-κB signaling pathway (90). Twist1 binds to E boxes present in the promoters of several NF-κB–dependent inflammatory cytokines, such as TNF-α, IL-1, and IL-6, and it suppresses cytokine production by blocking NF-κB–dependent transcriptional activation (38, 91). Sharif et al. reported the interaction between type I IFNs, Twist1, and the NF-κB pathway (39). They found that type I IFNs suppressed the production of TNF-α through the regulation of the expression of the receptor tyrosine kinase Axl and downstream induction of Twist1

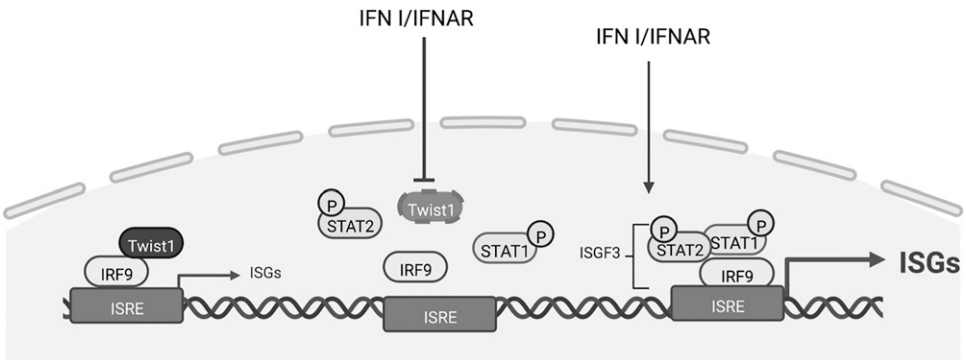

FIGURE 12. Twist–IRF9 interaction maintains basal ISG expression. Protein–protein interaction between Twist1 and IRF9 provides early protection against viral infections. Activation of the IFNAR pathway leads to Twist degradation and release of IRF9, allowing the interaction with p-STAT1 and p-STAT2 and formation of the ISGF3 complex.

(39); however, the type of interaction between Twist1 and type I IFN was not defined. Our findings revealed that as result of the type I IFN response to ZIKV, IFN-β inhibits Twist1 expression, a necessary step to mount a strong antiviral response; unfortunately, inhibition of Twist1 will also impact the capacity of the trophoblast to migrate and invade, two essential aspects for the success of the pregnancy.

In summary, we demonstrate that there is a direct interaction between Twist1 and IRF9, which leads to enhanced IRF9 transcriptional activity. To our knowledge, these findings demonstrate a novel mechanism of antiviral awareness necessary for an early response.

Acknowledgments

We thank Alyssa Alday for help with preparation of the manuscript.

Disclosures

The authors have no financial conflicts of interest.

References

1. Meizlish, M. L., R. A. Franklin, X. Zhou, and R. Medzhitov. 2021. Tissue homeostasis and inflammation. *Annu. Rev. Immunol.* 39: 557–581.
2. Kulkarni, O. P., J. Lichtnekert, H. J. Anders, and S. R. Mulay. 2016. The immune system in tissue environments regaining homeostasis after injury: is "inflammation" always inflammation? *Mediators Inflamm.* 2016: 2856213.
3. Shaykhiev, R., and R. Bals. 2007. Interactions between epithelial cells and leukocytes in immunity and tissue homeostasis. *J. Leukoc. Biol.* 82: 1–15.
4. Janeway, C. A., Jr. 2001. How the immune system protects the host from infection. *Microbes Infect.* 3: 1167–1171.
5. Iwasaki, A., and R. Medzhitov. 2010. Regulation of adaptive immunity by the innate immune system. *Science* 327: 291–295.
6. Ivashkiv, L. B., and L. T. Donlin. 2014. Regulation of type I interferon responses. *Nat. Rev. Immunol.* 14: 36–49.
7. Dutia, B. M., D. J. Allen, H. Dyson, and A. A. Nash. 1999. Type I interferons and IRF-1 play a critical role in the control of a gammaherpesvirus infection. *Virology* 261: 173–179.
8. Duncan, C. J. A., R. E. Randall, and S. Hambleton. 2021. Genetic lesions of type I interferon signalling in human antiviral immunity. *Trends Genet.* 37: 46–58.
9. Trinchieri, G. 2010. Type I interferon: friend or foe? *J. Exp. Med.* 207: 2053–2063.
10. Ding, J., A. Maxwell, N. Adzibolosu, A. Hu, Y. You, A. Liao, and G. Mor. 2022. Mechanisms of immune regulation by the placenta: role of type I interferon and interferon-stimulated genes signaling during pregnancy. *Immunol. Rev.* 308: 9–24.
11. Kell, A. M., and M. Gale, Jr. 2015. RIG-I in RNA virus recognition. *Virology* 479–480: 110–121.
12. Cavlar, T., A. Ablasser, and V. Hornung. 2012. Induction of type I IFNs by intracellular DNA-sensing pathways. *Immunol. Cell Biol.* 90: 474–482.
13. Stark, G. R., H. Cheon, and Y. Wang. 2018. Responses to cytokines and interferons that depend upon JAKs and STATs. *Cold Spring Harb. Perspect. Biol.* 10: a028555.
14. Gough, D. J., N. L. Messina, C. J. Clarke, R. W. Johnstone, and D. E. Levy. 2012. Constitutive type I interferon modulates homeostatic balance through tonic signaling. *Immunity* 36: 166–174.
15. Banninger, G., and N. C. Reich. 2004. STAT2 nuclear trafficking. *J. Biol. Chem.* 279: 39199–39206.
16. Wong, M. T., and S. S. Chen. 2016. Emerging roles of interferon-stimulated genes in the innate immune response to hepatitis C virus infection. *Cell. Mol. Immunol.* 13: 11–35.
17. Levy, D. E., D. S. Kessler, R. Pine, N. Reich, and J. E. Darnell, Jr. 1988. Interferon-induced nuclear factors that bind a shared promoter element correlate with positive and negative transcriptional control. *Genes Dev.* 2: 383–393.
18. Schoggins, J. W., S. J. Wilson, M. Panis, M. Y. Murphy, C. T. Jones, P. Bieniasz, and C. M. Rice. 2011. A diverse range of gene products are effectors of the type I interferon antiviral response. [Published erratum appears in 2015 *Nature* 525: 144.] *Nature* 472: 481–485.
19. Pestka, S., C. D. Krause, and M. R. Walter. 2004. Interferons, interferon-like cytokines, and their receptors. *Immunol. Rev.* 202: 8–32.
20. Taniguchi, T., and A. Takaoka. 2001. A weak signal for strong responses: interferon-alpha/beta revisited. *Nat. Rev. Mol. Cell Biol.* 2: 378–386.
21. Mor, G., P. Aldo, and A. B. Alvero. 2017. The unique immunological and microbial aspects of pregnancy. *Nat. Rev. Immunol.* 17: 469–482.
22. Costello, M. J., S. K. Joyce, and V. M. Abrahams. 2007. NOD protein expression and function in first trimester trophoblast cells. *Am. J. Reprod. Immunol.* 57: 67–80.
23. Abrahams, V. M., P. B. Aldo, S. P. Murphy, I. Visintin, K. Koga, G. Wilson, R. Romero, S. Sharma, and G. Mor. 2008. TLR6 modulates first trimester trophoblast responses to peptidoglycan. *J. Immunol.* 180: 6035–6043.
24. Abrahams, V. M., P. Bole-Aldo, Y. M. Kim, S. L. Straszewski-Chavez, T. Chaiworapongsa, R. Romero, and G. Mor. 2004. Divergent trophoblast responses to bacterial products mediated by TLRs. *J. Immunol.* 173: 4286–4296.
25. Abrahams, V. M., J. V. Fahey, T. M. Schaefer, J. A. Wright, C. R. Wira, and G. Mor. 2005. Stimulation of first trimester trophoblast cells with poly(I:C) induces SLPI secretion. *Am. J. Reprod. Immunol.* 53: 280.
26. Abrahams, V. M., Y. M. Kim, S. L. Straszewski, R. Romero, and G. Mor. 2004. Macrophages and apoptotic cell clearance during pregnancy. *Am. J. Reprod. Immunol.* 51: 275–282.
27. Abrahams, V. M., R. Romero, and G. Mor. 2005. TLR-3 and TLR-4 mediate differential chemokine production and immune cell recruitment by first trimester trophoblast cells. *Am. J. Reprod. Immunol.* 53: 279.
28. Racicot, K., J. Y. Kwon, P. Aldo, V. Abrahams, A. El-Guindy, R. Romero, and G. Mor. 2016. Type I interferon regulates the placental inflammatory response to bacteria and is targeted by virus: mechanism of polymicrobial infection-induced preterm birth. *Am. J. Reprod. Immunol.* 75: 451–460.
29. Kwon, J. Y., P. Aldo, Y. You, J. Ding, K. Racicot, X. Dong, J. Murphy, G. Glukshtad, M. Silasi, J. Peng, et al. 2018. Relevance of placental type I interferon beta regulation for pregnancy success. *Cell. Mol. Immunol.* 15: 1010–1026.
30. Silasi, M., I. Cardenas, J. Y. Kwon, K. Racicot, P. Aldo, and G. Mor. 2015. Viral infections during pregnancy. *Am. J. Reprod. Immunol.* 73: 199–213.
31. Yockey, L. J., K. A. Jurado, N. Arora, A. Millet, T. Rakib, K. M. Milano, A. K. Hastings, E. Fikrig, Y. Kong, T. L. Horvath, et al. 2018. Type I interferons instigate fetal demise after Zika virus infection. *Sci. Immunol.* 3: eaao1680.
32. Dudley, D. M., K. K. Van Rompay, L. L. Coffey, A. Ardeshir, R. I. Keesler, E. Bliss-Moreau, P. L. Grigsby, R. J. Steinbach, A. J. Hirsch, R. P. MacAllister, et al. 2018. Miscarriage and stillbirth following maternal Zika virus infection in nonhuman primates. *Nat. Med.* 24: 1104–1107.
33. van der Eijk, A. A., P. J. van Genderen, R. M. Verdijk, C. B. Reusken, R. Mögling, J. J. A. van Kampen, W. Widagdo, G. I. Aron, C. H. GeurtsvanKessel, S. D. Pas, et al. 2016. Miscarriage Associated with Zika virus infection. *N. Engl. J. Med.* 375: 1002–1004.
34. Schaub, B., A. Monthieux, F. Najihoullah, C. Harte, R. Césaire, E. Jolivet, and J.-L. Voluménie. 2016. Late miscarriage: another Zika concern? *Eur. J. Obstet. Gynecol. Reprod. Biol.* 207: 240–241.
35. Quicke, K. M., J. R. Bowen, E. L. Johnson, C. E. McDonald, H. Ma, J. T. O'Neal, A. Rajakumar, J. Wrammert, B. H. Rimawi, B. Pulendran, et al. 2016. Zika virus infects human placental macrophages. *Cell Host Microbe* 20: 83–90.
36. Lee, Y. B., I. Bantounas, D. Y. Lee, L. Phylactou, M. A. Caldwell, and J. B. Uney. 2009. Twist-1 regulates the miR-199a/214 cluster during development. *Nucleic Acids Res.* 37: 123–128.
37. Ahn, J. H., H. R. Park, C. W. Park, D. W. Park, and J. Kwak-Kim. 2017. Expression of TWIST in the first-trimester trophoblast and decidual tissue of women with recurrent pregnancy losses. *Am. J. Reprod. Immunol.* 78: e12670.
38. Zheng, S., M. Hedl, and C. Abraham. 2015. Twist1 and Twist2 contribute to cytokine downregulation following chronic NOD2 stimulation of human macrophages through the coordinated regulation of transcriptional repressors and activators. *J. Immunol.* 195: 217–226.
39. Sharif, M. N., D. Sosic, C. V. Rothlin, E. Kelly, G. Lemke, E. N. Olson, and L. B. Ivashkiv. 2006. Twist mediates suppression of inflammation by type I IFNs and Axl. *J. Exp. Med.* 203: 1891–1901.
40. Ding, J., P. Aldo, C. M. Roberts, P. Stabach, H. Liu, Y. You, X. Qiu, J. Jeong, A. Maxwell, B. Lindenbach, et al. 2021. Placenta-derived interferon-stimulated gene 20 controls ZIKA virus infection. *EMBO Rep.* 22: e52450.
41. Potter, J. A., M. Tong, P. Aldo, J. Y. Kwon, M. Pitruzzello, G. Mor, and V. M. Abrahams. 2020. Viral infection dampens human fetal membrane type I interferon responses triggered by bacterial LPS. *J. Reprod. Immunol.* 140: 103126.
42. You, Y., P. Stelzl, Y. Zhang, J. Porter, H. Liu, A. H. Liao, P. B. Aldo, and G. Mor. 2019. Novel 3D in vitro models to evaluate trophoblast migration and invasion. *Am. J. Reprod. Immunol.* 81: e13076.
43. Alexandrova, M., D. Manchorova, Y. You, G. Mor, V. Dimitrova, and T. Dimova. 2022. Functional HLA-C expressing trophoblast spheroids as a model to study placental-maternal immune interactions during human implantation. *Sci. Rep.* 12: 10224.
44. Sanjana, N. E., O. Shalem, and F. Zhang. 2014. Improved vectors and genome-wide libraries for CRISPR screening. *Nat. Methods* 11: 783–784.
45. Walter, D. M., O. S. Venancio, E. L. Buza, J. W. Tobias, C. Deshpande, A. A. Gudiel, C. Kim-Kiselak, M. Cicchini, T. J. Yates, and D. M. Feldser. 2017. Systematic in vivo inactivation of chromatin-regulating enzymes identifies Setd2 as a potent tumor suppressor in lung adenocarcinoma. *Cancer Res.* 77: 1719–1729.
46. Stewart, S. A., D. M. Dykxhoorn, D. Palliser, H. Mizuno, E. Y. Yu, D. S. An, D. M. Sabatini, I. S. Chen, W. C. Hahn, P. A. Sharp, et al. 2003. Lentivirus-delivered stable gene silencing by RNAi in primary cells. *RNA* 9: 493–501.
47. Straszewski-Chavez, S. L., V. M. Abrahams, A. B. Alvero, P. B. Aldo, Y. Ma, S. Guller, R. Romero, and G. Mor. 2009. The isolation and characterization of a novel telomerase immortalized first trimester trophoblast cell line, Swan 71. *Placenta* 30: 939–948.
48. Jeong, D. S., M. H. Kim, and J. Y. Lee. 2021. Depletion of CTCF disrupts PSG gene expression in the human trophoblast cell line Swan 71. *FEBS Open Bio* 11: 804–812.
49. Liu, H., L. Wang, Y. Wang, Q. Zhu, P. Aldo, J. Ding, G. Mor, and A. Liao. 2020. Establishment and characterization of a new human first trimester trophoblast cell line, AL07. *Placenta* 100: 122–132.
50. Visintin, I., Z. Feng, G. Longton, D. C. Ward, A. B. Alvero, Y. Lai, J. Tenthorey, A. Leiser, R. Flores-Saaib, H. Yu, et al. 2008. Diagnostic markers for early detection of ovarian cancer. *Clin. Cancer Res.* 14: 1065–1072.
51. Phipson, B., S. Lee, I. J. Majewski, W. S. Alexander, and G. K. Smyth. 2016. Robust hyperparameter estimation protects against hypervariable genes and improves power to detect differential expression. *Ann. Appl. Stat.* 10: 946–963.

52. Ritchie, M. E., B. Phipson, D. Wu, Y. Hu, C. W. Law, W. Shi, and G. K. Smyth. 2015. limma powers differential expression analyses for RNA-sequencing and microarray studies. *Nucleic Acids Res.* 43: e47.
53. Ahsan, S., and S. Draghici. 2017. Identifying significantly impacted pathways and putative mechanisms with iPathwayGuide. *Curr. Protoc. Bioinformatics* 57: 7.15.1–7.15.30.
54. Donato, M., Z. Xu, A. Tomoiaga, J. G. Granneman, R. G. Mackenzie, R. Bao, N. G. Than, P. H. Westfall, R. Romero, and S. Draghici. 2013. Analysis and correction of crosstalk effects in pathway analysis. *Genome Res.* 23: 1885–1893.
55. Draghici, S., P. Khatri, A. L. Tarca, K. Amin, A. Done, C. Voichita, C. Georgescu, and R. Romero. 2007. A systems biology approach for pathway level analysis. *Genome Res.* 17: 1537–1545.
56. Tarca, A. L., S. Draghici, P. Khatri, S. S. Hassan, P. Mittal, J. S. Kim, C. J. Kim, J. P. Kusanovic, and R. Romero. 2009. A novel signaling pathway impact analysis. *Bioinformatics* 25: 75–82.
57. Marini, F., and H. Binder. 2019. pcaExplorer: an R/Bioconductor package for interacting with RNA-seq principal components. *BMC Bioinformatics* 20: 331.
58. Gu, Z., R. Eils, and M. Schlesner. 2016. Complex heatmaps reveal patterns and correlations in multidimensional genomic data. *Bioinformatics* 32: 2847–2849.
59. Wickham, H. 2016. *ggplot2: Elegant Graphics for Data Analysis.* Springer, New York.
60. Edwards, R. G. 1988. Human uterine endocrinology and the implantation window. *Ann. N. Y. Acad. Sci.* 541: 445–454.
61. Edwards, R. G. 1995. Physiological and molecular aspects of human implantation. *Hum. Reprod.* 10(Suppl 2): 1–13.
62. Cross, J. C., M. Hemberger, Y. Lu, T. Nozaki, K. Whiteley, M. Masutani, and S. L. Adamson. 2002. Trophoblast functions, angiogenesis and remodeling of the maternal vasculature in the placenta. *Mol. Cell. Endocrinol.* 187: 207–212.
63. Adamson, S. L., Y. Lu, K. J. Whiteley, D. Holmyard, M. Hemberger, C. Pfarrer, and J. C. Cross. 2002. Interactions between trophoblast cells and the maternal and fetal circulation in the mouse placenta. *Dev. Biol.* 250: 358–373.
64. Aldo, P. B., M. J. Mulla, R. Romero, G. Mor, and V. M. Abrahams. 2010. Viral ssRNA induces first trimester trophoblast apoptosis through an inflammatory mechanism. *Am. J. Reprod. Immunol.* 64: 27–37.
65. Kovats, S., E. K. Main, C. Librach, M. Stubblebine, S. J. Fisher, and R. DeMars. 1990. A class I antigen, HLA-G, expressed in human trophoblasts. *Science* 248: 220–223.
66. Tilburgs, T. 2021. Presentation and recognition of placental, fetal, and pathogen-derived antigens in human pregnancy. In *Reproductive Immunology.* G. Mor, ed. Academic, London, U.K., p. 23–37.
67. Kraus, T. A., J. F. Lau, J.-P. Parisien, and C. M. Horvath. 2003. A hybrid IRF9-STAT2 protein recapitulates interferon-stimulated gene expression and antiviral response. *J. Biol. Chem.* 278: 13033–13038.
68. Paul, A., T. H. Tang, and S. K. Ng. 2018. Interferon regulatory factor 9 structure and regulation. *Front. Immunol.* 9: 1831.
69. Suprunenko, T., and M. J. Hofer. 2016. The emerging role of interferon regulatory factor 9 in the antiviral host response and beyond. *Cytokine Growth Factor Rev.* 29: 35–43.
70. Luker, K. E., C. M. Pica, R. D. Schreiber, and D. Piwnica-Worms. 2001. Overexpression of IRF9 confers resistance to antimicrotubule agents in breast cancer cells. *Cancer Res.* 61: 6540–6547.
71. Jiang, D. S., Y. X. Luo, R. Zhang, X. D. Zhang, H. Z. Chen, Y. Zhang, K. Chen, S. M. Zhang, G. C. Fan, P. P. Liu, et al. 2014. Interferon regulatory factor 9 protects against cardiac hypertrophy by targeting myocardin. *Hypertension* 63: 119–127.
72. Rauch, I., F. Rosebrock, E. Hainzl, S. Heider, A. Majoros, S. Wienerroither, B. Strobl, S. Stockinger, L. Kenner, M. Müller, and T. Decker. 2015. Noncanonical effects of IRF9 in intestinal inflammation: more than type I and type III interferons. *Mol. Cell. Biol.* 35: 2332–2343.
73. Huber, M., T. Suprunenko, T. Ashhurst, F. Marbach, H. Raifer, S. Wolff, T. Strecker, B. Viengkhou, S. R. Jung, H. L. Obermann, et al. 2017. IRF9 prevents $CD8^+$ T cell exhaustion in an extrinsic manner during acute lymphocytic choriomeningitis virus infection. *J. Virol.* 91: e01219-17.
74. Paun, A., and P. M. Pitha. 2007. The IRF family, revisited. *Biochimie* 89: 744–753.
75. Kessler, D. S., S. A. Veals, X. Y. Fu, and D. E. Levy. 1990. Interferon-alpha regulates nuclear translocation and DNA-binding affinity of ISGF3, a multimeric transcriptional activator. *Genes Dev.* 4: 1753–1765.
76. Maxwell, A. J., Y. You, P. B. Aldo, Y. Zhang, J. Ding, and G. Mor. 2021. The role of the immune system during pregnancy: General concepts. In *Reproductive Immunology.* G. Mor, ed. Academic, London, U.K., p. 1–21.
77. Marr, N., T. I. Wang, S. H. Kam, Y. S. Hu, A. A. Sharma, A. Lam, J. Markowski, A. Solimano, P. M. Lavoie, and S. E. Turvey. 2014. Attenuation of respiratory syncytial virus-induced and RIG-I-dependent type I IFN responses in human neonates and very young children. *J. Immunol.* 192: 948–957.
78. Shi, L., N. Tu, and P. H. Patterson. 2005. Maternal influenza infection is likely to alter fetal brain development indirectly: the virus is not detected in the fetus. *Int. J. Dev. Neurosci.* 23: 299–305.
79. Romero, R., J. Espinoza, L. F. Gonçalves, J. P. Kusanovic, L. Friel, and S. Hassan. 2007. The role of inflammation and infection in preterm birth. *Semin. Reprod. Med.* 25: 21–39.
80. Romero, R., Y. Xu, O. Plazyo, P. Chaemsaithong, T. Chaiworapongsa, R. Unkel, N. G. Than, P. J. Chiang, Z. Dong, Z. Xu, et al. 2018. A Role for the Inflammasome in Spontaneous Labor at Term. *Am. J. Reprod. Immunol.* 79: e12440.
81. Thirkill, T. L., K. Lowe, H. Vedagiri, T. N. Blankenship, A. I. Barakat, and G. C. Douglas. 2005. Macaque trophoblast migration is regulated by RANTES. *Exp. Cell Res.* 305: 355–364.
82. You, Y., P. Stelzl, D. N. Joseph, P. B. Aldo, A. J. Maxwell, N. Dekel, A. Liao, S. Whirledge, and G. Mor. 2021. TNF-α regulated endometrial stroma secretome promotes trophoblast invasion. *Front. Immunol.* 12: 737401.
83. George, J. S., R. Mortimer, and R. M. Anchan. 2022. The role of reproductive immunology in recurrent pregnancy loss and repeated implantation failure. In *Reproductive Immunology, Immunology of Recurrent Pregnancy Loss and Implantation Failure.* J. Kwak-Kim, ed. Academic, London, U.K., p. 223–240.
84. Hoen, B., B. Schaub, A. L. Funk, V. Ardillon, M. Boullard, A. Cabié, C. Callier, G. Carles, S. Cassadou, R. Césaire, et al. 2018. Pregnancy outcomes after ZIKV infection in French territories in the Americas. *N. Engl. J. Med.* 378: 985–994.
85. García-Sastre, A., and C. A. Biron. 2006. Type 1 interferons and the virus-host relationship: a lesson in détente. *Science* 312: 879–882.
86. Thisse, B., C. Stoetzel, C. Gorostiza-Thisse, and F. Perrin-Schmitt. 1988. Sequence of the twist gene and nuclear localization of its protein in endomesodermal cells of early Drosophila embryos. *EMBO J.* 7: 2175–2183.
87. Thisse, B., M. el Messal, and F. Perrin-Schmitt. 1987. The *twist* gene: isolation of a Drosophila zygotic gene necessary for the establishment of dorsoventral pattern. *Nucleic Acids Res.* 15: 3439–3453.
88. Bialek, P., B. Kern, X. Yang, M. Schrock, D. Sosic, N. Hong, H. Wu, K. Yu, D. M. Ornitz, E. N. Olson, et al. 2004. A Twist code determines the onset of osteoblast differentiation. *Dev. Cell* 6: 423–435.
89. Cheng, G. Z., W. Zhang, and L. H. Wang. 2008. Regulation of cancer cell survival, migration, and invasion by Twist: AKT2 comes to interplay. *Cancer Res.* 68: 957–960.
90. Li, S., S. E. Kendall, R. Raices, J. Finlay, M. Covarrubias, Z. Liu, G. Lowe, Y. H. Lin, Y. H. Teh, V. Leigh, et al. 2012. TWIST1 associates with NF-κB subunit RELA via carboxyl-terminal WR domain to promote cell autonomous invasion through IL8 production. *BMC Biol.* 10: 73.
91. Roberts, C. M., M. A. Tran, M. C. Pitruzzello, W. Wen, J. Loeza, T. H. Dellinger, G. Mor, and C. A. Glackin. 2016. TWIST1 drives cisplatin resistance and cell survival in an ovarian cancer model, via upregulation of *GAS6*, *L1CAM*, and Akt signalling. *Sci. Rep.* 6: 37652.